HHS Public Access

Author manuscript

J Med Chem. Author manuscript; available in PMC 2020 September 12.

Published in final edited form as:

J Med Chem. 2019 September 12; 62(17): 7618–7642. doi:10.1021/acs.jmedchem.9b00370.

Recent Progress in Natural-Product-Inspired Programs Aimed To Address Antibiotic Resistance and Tolerance

Yasmeen Abouelhassan, **Aaron T. Garrison**, **Hongfen Yang**, **Alejandra Chávez-Riveros**, **Gena M. Burch**, **Robert W. Huigens III***

Department of Medicinal Chemistry, Center for Natural Products, Drug Discovery and Development (CNPD3), College of Pharmacy, University of Florida, Gainesville, Florida 32610, United States

Abstract

Bacteria utilize multiple mechanisms that enable them to gain or acquire resistance to antibiotic therapies during the treatment of infections. In addition, bacteria form biofilms which are surface-attached communities of enriched populations containing persister cells encased within a protective extracellular matrix of biomolecules, leading to chronic and recurring antibiotic-tolerant infections. Antibiotic resistance and tolerance are major global problems that require innovative therapeutic strategies to address the challenges associated with pathogenic bacteria. Historically, natural products have played a critical role in bringing new therapies to the clinic to treat life-threatening bacterial infections. This Perspective provides an overview of antibiotic resistance and tolerance and highlights recent advances (chemistry, biology, drug discovery, and development) from various research programs involved in the discovery of new antibacterial agents inspired by a diverse series of natural product antibiotics.

Graphical Abstract

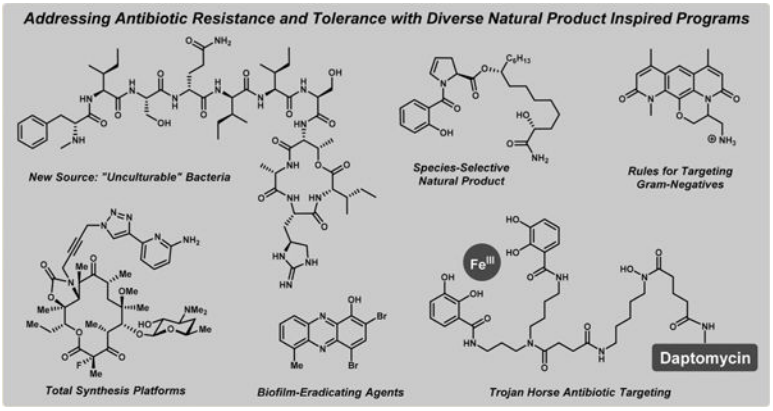

***Corresponding Author** rhuigens@cop.ufl.edu. Phone: (352) 273-7718.

The authors declare no competing financial interest.

INTRODUCTION

The discovery and routine administration of antibiotics to treat bacterial infections led to their recognition as “wonder drugs” in the mid-20th century.[1–9] To date, antibiotics are still considered one of the most significant interventions in human medicine. The efficacy and selectivity antibiotics exert made many believe that bacterial infections would be a thing of the past. However, instead of the routine eradication of bacterial pathogens in the clinic, we have witnessed an alarming rise in the failure to treat bacterial infections due to the generation of antibiotic-resistant “superbugs”[3,5] and antibiotic-tolerant persister cells and biofilms.[10–12]

Clinically approved antibiotics operate via the selective inhibition of critical targets that impede replication and growth or eradicate bacterial cells. It is interesting to note that relatively few bacterial targets have been exploited for antibiotic treatments in the clinic. The mechanisms of action for our arsenal of antibiotics include the inhibition or disruption of (1) cell wall synthesis (e.g., β-lactams,[13] vancomycin[14]), (2) protein synthesis (e.g., tetracyclines,[15] macrolides,[16] aminoglycosides,[17] linezolid[18]), (3) RNA poly-merase (e.g., rifamycins[19–21]), (4) nucleic acid synthesis (e.g., quinolones[22–25]), (5) folate biosynthesis (e.g., sulfonamides, trimethoprim),[26] and (6) cell membrane (e.g., polymyxins;[26] Figure 1).[4,7]

Upon exposure to antibiotics, bacteria can expediently evade their action using one or more well-defined resistance mechanisms.[3–6,8,27,28] Bacterial resistance has led to the catastrophic rise of roughly 2 million annual infections, resulting in 23 000 deaths in the United States.[29] In Europe, more than 33 000 deaths were attributed to antibiotic-resistant bacterial infections in 2015.[30] Universal acquired resistance mechanisms can prevent antibiotics access to the aforementioned intracellular targets. The cell wall of Gram-negative bacteria consists of inner and outer membranes, which upon mutation can act as a permeability barrier to antibiotics leading to reduced penetration into the cells.[31,32] Alternatively, bacteria can actively eliminate, or “pump out”, antibiotics before they bind their corresponding intracellular target via the action of efflux pumps (e.g., efflux of macrolides).[31,32] Mutations and modifications of the target’s binding site are, collectively, another resistance mechanism bacteria utilize to acquire resistance as the resulting changes negatively impact drug–target interactions of antibiotic therapies. Specific examples of mutation and modification to impede antibiotic binding sites include (1) mutation and alteration of penicillin binding proteins to negate the effects of penicillin, (2) structural alterations in DNA gyrase to prevent fluoroquinolone action, and (3) methylation of critical residues within the rRNA of bacterial ribosomes to eliminate the binding of aminoglycosides.[33–35] Additionally, bacteria can enzymatically modify antibiotics to generate inactive agents, and examples include (1) hydrolysis of β-lactam antibiotics by β-lactamase enzymes to cleave and destroy the critical β-lactam warhead (pharmacophore) required for antibacterial activities and (2) modification, or functionalization (e.g., acylation), of hydroxyl and/or amine groups critical for aminoglycoside antibiotics to hydrogen bond (bind) to bacterial ribosomes by aminoglycoside-inactivating enzymes.[29] In addition, bacteria can overproduce targets to bypass the effects of antibiotics (e.g., trimethoprim; Figure 1).[29,35]

Innate antibiotic tolerance is a distinct microbiological phenomena from acquired resistance and is now recognized as the underlying cause of chronic and recurring bacterial infections.[36] Using a communication process known as quorum sensing, bacteria secrete and sense small organic signaling molecules to monitor their population density and coordinate virulent behaviors.[37–41] Bacteria use quorum sensing to coordinate surface attachment and subsequent biofilm formation, where dense communities of bacterial cells are encased within matrixes of polysaccharides and extracellular DNA.[42–46] Once within a biofilm, bacterial cells divide at a much slower rate compared to their planktonic (free-floating) counterparts or they do not replicate at all. The subpopulation of biofilm cells that enter into a dormant state are known as “persister cells” and are characterized as metabolically inactive.[12,47–51] Extracellular polymeric substances (EPSs), or biofilm matrix, provide an additional layer of protection to surface-attached communities, enabling these bacteria to thrive in harsh conditions (e.g., host immune response).[52,53]

It is important to note that all classes of FDA-approved conventional antibiotics were initially discovered as bacterial growth inhibitors against actively dividing cultures. Therefore, it should be no surprise that clinically used antibiotics are essentially ineffective against nonreplicating biofilm infections. With the 17 million new cases of biofilm infections in addition to >500 000 deaths each year in the United States that result from these infections, there is a critical need to identify compounds that effectively eradicate biofilms through growth-independent mechanisms (Figure 2).[10,41]

The current need for new and effective antibiotic therapies has motivated several research groups to initiate drug discovery programs inspired by various antibiotic natural products, which may be known or recently discovered. The Lewis group has created a new technology to facilitate isolation of novel antibiotics from previously inaccessible sources, while the Myers lab has developed novel total synthesis platforms for the discovery of new antibiotics. The Hergenrother group elegantly utilized a collection of diverse small molecules to establish guidelines that will allow the targeting of clinically imposing Gram-negative pathogens. The Miller group has pioneered a Trojan horse strategy and continues to make advances in this area by taking advantage of siderophore systems for bacterial import in unique and elegant ways to impart activity against Gram-negative organisms. Recent work by the Wuest lab has focused on a natural product with narrow-spectrum activity against *Pseudomonas aeruginosa*. Both broad- and narrow-spectrum-based strategies have been employed, but scientists agree that care must be taken to minimize resistance development against these novel agents. With biofilms being inherently tolerant to current antibiotics, the Lewis group and our lab have identified agents capable of eradicating persister cells and established biofilms. Our group has identified a series of synthetically tunable halogenated phenazine small molecules derived from a marine antibiotic that potently eradicates bacterial biofilms through a rapid iron starvation mechanism. Fortunately, recent advances in chemistry, molecular biology, and chemical biology have yielded a bevy of powerful techniques that can be employed to better understand problems associated with pathogenic bacteria and enable the discovery of novel natural-product-inspired therapies. This Perspective will detail each of these innovative and exciting antibiotic discovery strategies (Figure 3).

TEIXOBACTIN, A PROMISING NEW ANTIBIOTIC: iChip DISCOVERY, TOTAL SYNTHESIS, AND NOVEL ANALOGUES

Bacteria compete for finite resources in their environment and often produce antibiotics to compete with each other. Many antimicrobials used in the clinic today have been derived from natural products produced by bacteria. Large numbers of organisms cannot be grown successfully through traditional culturing methods and are thus named “unculturable”.[1] It is believed that approximately 99% of all species in external environments are uncultured.[54] However, recent development of iChip technology by the Lewis group has enabled the growth of previously uncultured bacteria (Figure 4).[54,55] This new technology has enhanced the potential for many more types of bacteria to be investigated and screened for the identification of new antibiotics.

By use of the iChip, extracts from 10 000 bacterial isolates were grown and screened, which led to one isolate (β-proteobacteria, named *Eleftheria terrae*) that demonstrated antibacterial activity against *S. aureus*. From the *Eleftheria terrae* extract, teixobactin **1** was isolated and structurally elucidated using mass spectrometry, NMR, and Marfey’s analysis.[55] Teixobactin **1** proved to be a unique antibiotic containing a cyclic depsipeptide moiety composed of four amino acid residues, including an enduracididine residue, that are appended to a seven amino acid linear chain bearing a methylphenylalanine. It is also interesting to note that **1** has four D-amino acid residues incorporated into its impressive structure. The biosynthetic gene cluster consists of two nonribosomal peptide synthetase (NRPS) genes named *txo1* and *txo2* where 11 modules are encoded. The depsipeptide 1 showed excellent antibacterial activities in minimum inhibitory concentration (MIC) assays against significant, Gram-positive pathogens, including *S. aureus* (MIC = 0.25 μg/mL against methicillin-sensitive and methicillin-resistant strains; **1** also demonstrated antibacterial activities against intermediate vancomycin-resistant *S. aureus*, VISA), enterococci (MIC = 0.5 μg/mL, vancomycin-resistant enterococci strains, VRE), *M. tuberculosis* (MIC = 0.125 μg/mL), *Clostridium dif f icile* (MIC = 0.005 μg/mL), and *Streptococcus pneumoniae* (MIC ≤ 0.03 μg/mL, penicillin-resistant strain) as reported by Lewis and co-workers.[54]

A common technique for determining the mechanism of action for antibiotics is to generate resistant mutants. Lewis and colleagues were not able to develop resistant mutants of *S. aureus* or *M. tuberculosis*, indicating that teixobactin’s target may not be a protein. This hypothesis was supported by the inhibition of peptidoglycan synthesis by **1**, while no effect was observed on biosynthesis of DNA, RNA, or proteins. Because true vancomycin resistance in *S. aureus* is rare and vancomycin is known to bind lipid II, Lewis and co-workers hypothesized that teixobactin could also exert its activity through interaction with this target. When whole cells (*S. aureus*) were treated with **1**, a significant amount of the peptidoglycan precursor undecaprenyl-*N*-acetylmuramic acid-pentapeptide (UDP-Mur-NAc-pentapeptide) accumulated in a similar fashion to cells treated with vancomycin. Competition enzyme binding assays indicated that **1** does not inhibit MurG, FemX, or PBP2 enzymes directly, while the addition of lipid II prevented **1** from inhibiting growth against *S. aureus*. These combined results demonstrate that **1** specifically interacts with the peptidoglycan precursor rather than interfering with the activity of the enzymes. Teixobactin

retained activity against VRE which has a modified lipid II, suggesting that it binds at a different site than vancomycin.[54]

The therapeutic potential of **1** was also reported by Lewis and co-workers.[54] Teixobactin retained its antibacterial potency in the presence of serum and demonstrated good chemical and microsomal stability and low toxicity. The pharmacokinetic parameters showed that after a single 20 mg per kg dose (iv injection) of **1** in mice, serum concentrations were maintained above MIC values for 4 h. Animal efficacy studies were then performed with **1** in a mouse septicemia model against MRSA at a dose that leads to 90% death; however, treatment with **1** (iv at 20 mg/kg, 1 h after infection) resulted in the survival of all mice, and a later experiment determined the PD_{50} (protective dose at which half of the animals survive) of **1** to be 0.2 mg/kg. **1** was also shown to be efficacious in a thigh infection of *S. aureus* and a lung infection model of *S. pneumoniae*, causing a 6 $\log_{10}$ reduction of colony forming units (CFU) per mL.[54]

Following the initial report of teixobactin's discovery, two total syntheses of **1** have been published utilizing solid-phase technology in separate reports by Payne and co-workers[56] and Li and co-workers.[57] In both total syntheses of **1**, macro-lactamization at the less hindered Thr_8-Ala_9 connection has proved to be the fruitful cyclization approach (see conversion of **5** to **6**, Figure 5A, by Li and co-workers) as opposed to a macrolactonization strategy. Following the macrolactamization step, Li and co-workers coupled linear peptide **3** to cyclic peptide **6** using a key ligation step in pyridine/acetic acid before final HPLC conversion to **1**. Yuan and co-workers developed a stereoselective and scalable synthetic route to the rare L-*allo*-enduracididine (L-*allo*-End)[58] moiety of **1**, which played a critical role in the total synthesis reported by Li and co-workers.

In addition to total synthesis campaigns, solid-phase chemistry has enabled initial medicinal chemistry efforts of **1** by multiple groups, including Albericio,[59] Singh,[60–63] Su and Fang,[64] Rao,[65] Li,[66] and Chan.[67] Several of these groups have probed the structural requirements of the L-*allo*-enduracididine moiety at position 10 of **1**. If this unique residue is not required for antibacterial activities, then more simplified analogues of **1** can be prepared more readily. Albericio and co-workers were the first to report the replacement of the unusual L-*allo*-enduracididine residue of **1** by substituting with L-arginine; however, this new analogue lost significant antibacterial activities against *S. aureus* (MIC = 1.6 μg/mL) and *B. subtilis* (MIC = 0.40 μg/mL) based on MIC value comparison (**1** reported MIC values with ≥8-fold more potent activities when compared to this analogue).[59] Fang and Su and co-workers synthesized nine teixobactin analogues, which establish that (1) a guanidine or amine group at position 10, (2) the hydroxyl group of serine (position 7), (3) the N–H proton of the terminal phenylalanine (position 1) were all critical for antibacterial activity. During these investigations, Fang and Su also reported that position 4 can tolerate various side chain size and functional group content.[64]

The initial reports of teixobactin analogues gave insightful information into the SAR of **1**; however, a "first wave" of synthetic analogues reported by Albericio, Su, Fang, and co-workers[59,64] lost a substantial amount of antibacterial activity and appeared to be less than exciting lead molecules. Rao and co-workers[65] recently reported the synthesis of 21 new

teixobactin analogues, including simplified and equipotent analogue **7** (Figure 5B). This work demonstrated that the *N*-Me-D-Phe residue at position 1 of teixobactin (1) tolerates additional hydrophobic groups on the phenyl ring and (2) does not require the methyl group on the amine, as the primary amine was well tolerated. These structural modifications combined with a L-lysine substitution of the L-*allo*-enduracididine residue at position 10 resulted in equipotent analogue **7**, which also demonstrated outstanding in vivo efficacy in a *S. pneumonia* mouse model of infection (100% survival rate of mice infected with bacterial loads that lead to 90% death in controls).

DEFINING RULES TO TARGET GRAM-NEGATIVE BACTERIA AND CONVERTING A DEOXYNYBOMYCIN ANALOGUE TO A BROAD-SPECTRUM ANTIBIOTIC

Gram-negative pathogens are a major clinical problem due to their lack of sensitivity to many commonly used anti-biotics.[68,69] Quinolones were the last new class of antibacterial agents active against Gram-negative bacteria introduced into the clinic in 1968.[1] Despite extensive high-throughput screening efforts against *Escherichia coli* with large compound libraries of synthetic compounds, no lead compounds were translated into clinical agents.[70] With two cellular membranes and a lipopolysaccharide-coated outer membrane, Gram-negative bacteria pose significant challenges for compound entry.[68,71–73] Compounds capable of penetrating the outer membrane do so through porins, which are narrow trans-membrane proteins lined with charged amino acids. Once inside Gram-negative bacterial cells, small molecules are susceptible to removal through the function of efflux pumps; therefore, in order for a compound to accumulate within Gram-negative bacteria and engage its intracellular target, compounds are required to enter through porins faster than being removed via efflux.[68]

Hergenrother and co-workers noted that despite initial efforts by others, we have a limited understanding of the physicochemical properties enabling compound accumulation in Gram-negative bacteria.[68,72,73] A structurally diverse set of 100 compounds with unique scaffolds rapidly accessed from available natural products were used to systematically analyze small molecule accumulation in *E. coli* (whole cells) using a liquid chromatography with tandem mass spectroscopy (LC–MS/MS) method. This approach using whole cells allowed multiple variables affecting compound accumulation to be accounted for, such as multiple porins, efflux pumps, and lipopolysaccharide composition. Conventional antibiotics with known high (i.e., tetracycline) and low (i.e., novobiocin) accumulation properties were evaluated as controls and reported to validate the method.[68]

Natural-product-derived compounds were selected for this study as most clinically used antibacterial drugs are either natural products or derivatives. The compound collection utilized by the Hergenrother lab was synthesized by this team, so these compounds are synthetically accessible with tunable properties to enable structure–activity relationships geared toward accumulation in Gram-negative bacteria. The library of 100 compounds utilized for this work, which was generated utilizing the “complexity-to-diversity” approach,[74–78] included positively charged, negatively charged, and neutral compounds.[68] The

chemical structure, molecular weight, $ClogD_{7.4}$, and charge of all compounds were tracked with accumulation results in *E. coli*.

From the initial accumulation studies, the primary factor that governed accumulation in *E. coli* was charge, with 12 of 41 positively charged compounds being the most likely to accumulate. Interestingly, 8 of the 12 positively charged compounds were primary amines.[68] In follow-up SAR investigations, replacement of the primary amine with different functional groups (e.g., carboxylic acid, amide, alcohol) or amines bearing more substitutions significantly reduced accumulation in *E. coli*. Although the presence of a primary amine was important for accumulation, it alone was insufficient; therefore, chemoinformatics was utilized to understand which factors contribute to amine accumulation. This work revealed that the flexibility, as measured by the number of rotatable bonds, and shape of a compound are important factors that govern accumulation. Compound shape was described by "globularity" to inform the three-dimensionality. Shape was scored on a scale from 0 globularity for a "flat" compound (e.g., benzene) to 1 globularity for a "spherical" compound (e.g., adamantane).

On the basis of the extensive data set generated by Hergenrother and co-workers, the following guiding principles for accumulation in *E. coli* were developed: (1) compounds are most likely to accumulate if they contain a nonsterically encumbered amine, (2) contain some nonpolar functionality (typically not a problem for organic compounds), (3) contain a rigid structure and (4) have low globularity.[68] These guidelines are referred to as the "eNTRy rules" (N, ionizable nitrogen, primary amine is best; T, low three-dimensionality, globularity score of ≤0.25; R, relatively rigid, ≤5 rotatable bonds).[73] These guidelines were validated retrospectively with antibacterial agents presented by O'Shea and Moser.[79] In addition, the role of porins was examined by testing the high-accumulation antibiotic controls and test compounds in a strain bearing a diminished number of porins.[68] As predicted, a decrease in accumulation was observed for all compounds tested in the strain with fewer porins. Molecular modeling was performed with select test compounds and antibacterial agents that transverse the major porin of *E. coli*, OmpF, revealing a key interaction between the necessary primary, or non-hindered, amine and acidic residues (most often Asp113) that allow high accumulating compounds.

These well-defined guidelines were instructive in converting an analogue of the Gram-positive antibiotic deoxynybomycin (DNM, **9**) into the broad-spectrum agent, 6DNM-NH3 (**11**, Figure 6).[68] DNM is an inhibitor of DNA gyrase,[80] however, only active against Gram-positive pathogens, presumably due to minimal accumulation in Gram-negative bacteria.[68] DNM possesses shape and rigidity features that align with the eNTRy rules; however, no amine group is present. Analogue 6DNM **10** possesses an aliphatic bridge expanded by one methylene unit to give a six-membered ring, compared to DNM's (9) five-membered ring.

As one would expect based on the small structural differences between analogues, DNM **9** and 6DNM **10** possess the same activity profile (*S. aureus* MIC = 0.06–1 μg/mL; *E. coli* MIC > 32 μg/mL). However, 6DNM-NH3 **11** has incorporated a primary amine appended to the aliphatic region of the six-membered ring, and as predicted based on the eNTRy rules, **11** demonstrates significantly higher levels of accumulation compared to 6DNM **10** (**11**,

accumulation = 1114 nmol per 1012 CFU; 10, accumulation = 298 nmol per 10^{12} CFU). In line with eNTRy rule design and observed increases regarding *E. coli* accumulation, 6DNM-NH3 demonstrates broad-spectrum antibacterial activities (**11**, *S. aureus* MIC = 0.03–0.5 μg/mL; *E. coli* MIC = 0.5–16 μg/mL), including activities against several Gram-negative pathogens (**11**, *A. baumannii* MIC = 2–16 μg/mL; *K. pneumoniae* MIC = 1–8 μg/mL; *E. cloacae* MIC = 0.5–4 μg/mL; *P. aeruginosa* MIC = 16 μg/mL).[68] Steered molecular dynamics simulations indicated that 6DNM-NH3 **11** was able to pass through the porin OmpF with the assistance of the key interaction between the primary amine of **11** and Asp113 within the porin channel; however, 6DNM **10** was incapable of this interaction and required distortion in Asp113 and neighboring residues to allow passage. This ground-breaking work will undoubtedly pave the way for the discovery and development of antibiotics against Gram-negative pathogens.[72]

DEVELOPING TOTAL SYNTHESIS PLATFORMS FOR NEW, FULLY SYNTHETIC ANTIBIOTICS

One of the primary methods to discover and develop new antibacterial agents over the past 60 years has been semisynthesis, which is chemical synthesis using natural products (e.g., antibiotics) as starting points.[81] Early examples of semisynthesis in the antibacterial arena include the conversion of (1) streptomycin to dihydrostreptomycin (via a chemoselective reduction of the aldehyde in streptomycin to a primary alcohol to yield a new, more stable antibacterial agent) and (2) chlorotetracycline to tetracycline (via hydro-genation; tetracycline was later isolated). With these early success stories, medicinal chemists realized the value of semisynthesis for antibacterial discovery and utilized this approach to advance other antibiotic classes (e.g., macrolides, synthetic transformation of erythromycin to azithromycin in four steps); however, this approach has significant limitations as deep-seated modifications are not always accessible via semisynthesis. Myers and co-workers are working to address these limitations by developing modular total synthesis platforms, and they have made significant progress generating novel tetracycline[81–88] and macrolide antibiotics[89–93] bearing structural modifications not possible through current semisynthetic approaches.

In the mid-1990s, the Myers lab began work on fully synthetic tetracycline antibiotics.[82] This program led to the implementation of a high-yielding, diastereoselective Michael–Claisen annulation between benzoate esters related to **13** and chiral “AB enone” **14**, resulting in the constructive C-ring “stitching” of new tetracycline antibiotics.[81–86] The “diversity element” of this route can be clearly seen in structure **15** (Figure 7), which bears four positions poised for structural modification. On the basis of structure–activity relationship knowledge, the diversity element tracks to positions that do not negatively impact bacterial ribosome inhibition by tetracyclines. This incredible chemistry platform has enabled >3000 fully synthetic tetracyclines to date,[81,82,86] several of which have proven to be promising clinical candidates (e.g., **24, 25**) including ervacycline **26** (XERAVA), which recently received FDA approval for the treatment of complicated intra-abdominal infections (cIAI).[94] As presented in Figure 7D, ervacycline **26** has very potent, broad-spectrum activity against several pathogenic bacteria, including methicillin-resistant *Staphylococcus aureus*.

The Myers lab has also recently established a total synthesis platform for the discovery of new macrolide antibiotics.[89–93] Myers and co-workers reported the generation of >300 fully synthetic macrolides (FSMs) that incorporate structural design features that combine structure–activity relationship knowledge (macrolactone, C9 ketone/amine replacement, 14- or 15-membered macrocycle, incorporation of desosamine sugar at C5) with resistance liabilities (replacement of C3-clasinose sugar with ketone to give ketolides; Figure 8A) to inform the synthesis of new macrolides.[92] Eight simple building blocks (**30**–**33**, **38**–**40**, **47**; Figure 8B) were utilized to assemble key left-handed fragment **44** (amine) and right-handed fragment **43** (ketone), which were then joined, or converged, through a stereoselective reductive amination reaction followed by sequential macrolactonization and click reactions to yield **48** (a 14-membered azaketolide). The Myers team noted that many past macrolide synthesis efforts have failed at the critical macrolactonization step; therefore, special attention was made to rigidify the substrate via the cyclic carbamate group, which led to an impressive 78% yield for the macrolactonization step (on gram scale). Several clinically effective and promising macrolides have cyclic carbamate moieties fused to the C12/ C13 position of the macrolide, including telithromycin, cethromycin, and solithromycin **50**. An additional benefit of the cyclic carbamate moiety is that the aniline residue of solithromycin **50** is known to bind a unique pocket in the bacterial ribosome,[92] making such structures better inhibitors of this target and more effective antibacterial agents.

A series of 15-membered azaketolides, including FSM **49**, was synthesized using a similar route to the 14-membered azaketolides (Figure 8B).[92] This new route required modification to only three of the building blocks (**34**, **35**, and **41**, the original glycosyl donor reported by Woodward et al.[95]) used to synthesize the 14-membered azaketolides. The key left-handed fragment **44** was also utilized in this route and underwent an analogous (1) reductive amination with right-hand aldehyde **45**, (2) macrolactonization (94% yield, 1.9 g scale), (3) click reaction sequence to afford 15-membered azaketolide **49**. Myers and co-workers also utilized the key right-hand aldehyde **45** to access a series of 14-membered ketolides, including the clinical candidate solithromycin **50** and approved drug telithromycin (not shown). Intermediate **42**, which was accessed through a stereoselective addition of ketone **36** with alkynyl lithium **37**, was transformed into a Grignard reagent via the hydromagnesiation of the acetylenic moiety and subsequently reacted with aldehyde **45** to join the key left- and right-hand fragments of the ketolide series. Following a subsequent oxidation/deprotection sequence, the key macrolactionization step was successfully carried out in 66% yield (1.7 g scale) to produce the desired 14-membered macrolactone scaffold. A final reaction sequence involving C2 fluorination and installation of the cyclic carbamate (bearing the important aniline residue) led to the synthesis of solithromycin **50** in **14** steps and 16% yield from **34** and **35**.

This total synthesis platform was utilized to generate >300 FSM antibiotic candidates by varying building blocks in addition to modifying readily diversifiable structural features at multiple positions around the macrolactone architecture.[92] This proved to be a powerful synthetic medicinal chemistry tactic as deep-seated variations at select positions within FSM scaffolds were accessed, which are not possible using semisynthetic approaches. Following chemical synthesis, 305 FSMs were evaluated for antibacterial activities against a diverse

panel of Gram-positive and Gram-negative pathogens. Potent antibacterial agents were identified among each of the FSM subclasses (14-membered azaketolides, 15-membered azaketolides, 14-membered ketolides).

Following the initial screen, the most promising FSMs were evaluated against an expanded panel of bacteria with genetically characterized resistance mechanisms to erythromycin (*ermB*, ribosome-modifying methyltransferase; *mefA*, efflux; Figure 9) and other antibiotics (MRSA and VRE strains).[92] Several analogues (e.g., **49**, **51**, **52**; Figure 9) demonstrated significant improvements in activity against this macrolide-resistant panel of pathogenic bacteria. FSM **51** (FSM-100573) is a 14-membered ketolide that demonstrated remarkable activities during these investigations. In fact, **51** outperformed every current clinically used macrolide antibiotic against extremely challenging strains, such as *S. pneumoniae* with both *ermB* and *mefA* genes. FSM **51** also demonstrated significant improvements against Gram-negative pathogens, such as *A. baumannii* and *P. aeruginosa*.

This incredible synthesis platform has created unprecedented opportunities to explore and develop novel macrolide antibiotics. The synthesis approach to FSMs is highly convergent from multiple building blocks; however, key advanced left-handed and right-handed intermediates were strategically utilized in divergent pathways to access multiple FSM subclasses (e.g., left-handed fragment 44 was used to synthesize 14- and 15-membered azaketolide scaffolds; right-handed fragment **45** was used to synthesize 15-membered azaketolide and 14-membered ketolide scaffolds). Similar to Myers' tetracycline synthesis platform, one can envision accessing thousands of FSM from the chemistry described here. Myers and co-workers have truly inspired scientists and clinicians with this ground-breaking work, which has great potential to lead to new clinical agents that overcome bacterial resistance in human patients.

PROMYSALIN: A SPECIES-SPECIFIC ANTIBIOTIC THAT TARGETS SUCCINATE DEHYDROGENASE IN *Pseudomonas aeruginosa*

Broad-spectrum antibiotics target essential pathways in bacteria, including cell wall and protein synthesis, and are capable of treating a wide range of infections.[96] However, misuse and prolonged exposure to broad-spectrum antibiotics can result in undesirable side effects (e.g., inflammatory diseases, obesity) as commensal population dynamics can be dramatically altered by these agents.[96–98] "Narrow-spectrum" antibiotics (e.g., amoxicillin) target large subsets of bacteria, such as Gram-positive versus Gram-negative bacteria, or anaerobes versus aerobes; however, species-specific agents against significant human pathogens would be extremely useful and could avoid the undesired side effects that result from the misuse of our current antibiotic arsenal.[96]

Over the past several years, Wuest and co-workers have developed an exciting medicinal chemistry and chemical biology program around the species-selective agent promysalin **53** (Figure 10A), which targets the major Gram-negative pathogen *Pseudomonas aeruginosa*.[96,99–103] The multispecies community found in the root systems of various plants is known as the rhizosphere,[104,105] and in this environment, bacteria are known to utilize chemical warfare strategies for colonization and to defend themselves. *Pseudomonads* are highly

prevalent in the rhizosphere, and these bacteria produce an array of secondary metabolites with biological activities that promote survival, including antibiotics, virulence factors, biosurfactants, siderophores (to obtain iron from their environment).[99] Promysalin is a secondary metabolite isolated from *Pseudomonas putida* found in rice plants.[106] This natural product induces swarming and biofilm formation in *P. putida*; however, it demonstrates unique species-specific antibacterial activity against *P. aeruginosa* (growth inhibition, IC_{50} = 0.83 μg/mL; note, MIC values have not been reported for the promysalin work described here).

Wuest and co-workers reported a convergent and concise total synthesis of (−)-promysalin **53** (Figure 10).[99] In the original isolation paper by De Mot and co-workers,[106] the three stereogenic centers of promysalin were not defined. Therefore, Wuest's total synthesis of promysalin involved a unique combination of bioinformatics (reannotation of the biosynthetic gene cluster via AntiSMASH computation) and stereoselective approaches (reagent control, substrate selection; Figure 10B) to yield four diastereomers of promysalin for structural elucidation and biological assessment.

All four diastereomers of the myristic acid fragment **60** (diastereomers **60a–d**) of promysalin were synthesized using a stereoselective, five-step synthetic route.[99] First, Evans' oxazolidinone **54** underwent a diastereoselective hydroxylation (oxidation) upon treatment with sodium hexamethyldisilazane followed by addition Davis oxaziridine **58**, then a TBS-protection afforded **59**. This was followed by a cross-metathesis reaction with homoallylic alcohol **55**, and then hydrogenation of the resulting olefin (not shown) and final ammonolysis of the oxazolidinone moiety with ammonium hydroxide afforded amide **60**. EDC-coupling of the alcohol in **60** with acid (−)-**62** and then silyl-group removal with tetrabutylammonium fluoride afforded promysalin **53**. All four diastereomers of **60** (**60a–d**) were synthesized and coupled to (−)-**62** to afford all possible diastereomers at C2 and C8 of the myristic acid moiety of promysalin (**53a–d**).

With the four diastereomers of **53** in hand, NMR comparison and antibacterial assays were utilized in concert to unequivocally identify diastereomer **53a** as the natural product. Unfortunately, no optical rotation or authentic sample was available to compare; however, Wuest and co-workers rationalized that the correct enantiomer would exhibit the most potent biological activity.[99] Promysalin **53a**, which had identical spectral data to those reported in De Mot's isolation paper, proved to have the most potent antibacterial activities against *P. aeruginosa* strain *PA14*, which demonstrated an IC_{50} value of 125 nM (IC_{50} = 1.8 μM, initial report) and an IC_{50} value of 1 μM against *PAO1*. The other diastereomers **53b–d** demonstrated >10-to >60-fold less potency against *P. aeruginosa* strain *PA14* than **53a**. On the basis of these findings, the absolute stereochemistry of natural promysalin (−)-**53** was assigned as (2*R*,8*R*,16*S*).

By use of the total synthesis of promysalin **53** as a platform, a series of 16 related analogues was generated via diverted total synthesis.[96] This approach allowed several structural features to be probed (i.e., ester linker, proline ring size and functionality, hydroxyl group on the myristic acid fragment) to gain structure–activity relationship information regarding **53**. From these investigations, several interesting structural features were identified that led to a

complete abolishment of antibacterial activity against *PA14*, including (1) proline ring size and saturation (analogue **63**) and (2) substitution of the ester group with an amide (analogue **64**). In contrast, removal of the C2 hydroxyl group (analogue **65**) and introduction of a vinyl fluoride on the proline moiety (analogue **66**) resulted in promysalin analogues with improved antibacterial activities against *PA14*.

The SAR insights gained from the diverted synthesis of promysalin analogues enabled the design, synthesis, and utilization of diazirine photoprobe **67**, which retained activity, in affinity-based protein profiling (AfBPP) studies.[101] Active promysalin photoprobe **67**, inactive photoprobe 68 (to identify nonspecific protein binding partners), and promysalin (for competition purposes) were utilized in an elaborate series of experiments (involving irradiation of photoactive probes in cell lysate, subsequent click reaction with biotin azide, pull-down, dimethyl isotope labeling, and LC–MS/MS measurement; Figure 11) that led to the identification of succinate dehydrogenase (SdhC) as the target of promysalin. Further validation that SdhC was the target of **53** was carried out in vitro and via whole genome sequencing of resistant mutants. These findings demonstrate that targeting the tricarboxylic acid (TCA) cycle could be useful in developing narrow, species-selective antibiotic therapies and warrant additional studies regarding SdhC as an antibiotic target.[101–103]

RECENT ADVANCES OF SIDEROPHORE CONJUGATES FOR “TROJAN HORSE” TARGETED DELIVERY OF ANTIBIOTICS TO PATHOGENIC BACTERIA

Bacteria are able to successfully establish an infection when they experience unlimited growth and proliferation within a host.[107] In order for bacteria to proliferate, adequate supply of key nutrients is required. Iron is a crucial nutrient that bacteria require to thrive and is known to play critical roles in energy metabolism, stabilization of protein structures, and oxygen transport.[107–109] Unfortunately, iron is not membrane soluble and, therefore, is unable to diffuse through bacterial membranes, so acquisition of this key nutrient has its challenges; however, bacteria synthesize and utilize specialized organic molecules known as siderophores to acquire iron from their surroundings.[107,108] Bacteria secrete specific siderophores into their environment where they tightly bind iron(III). The resulting iron(III)-siderophore complex is then recognized by specific cell-surface receptors on bacteria, which shuttles the complex inside the bacterial cell. Once within the reductive cytoplasm of the bacterium, iron(III) is reduced to iron(II), resulting in a loss of affinity by the siderophore and subsequent release of iron(II) for unitization by the bacterial cell.[107]

Bacteria utilize highly specific siderophore systems that can be exploited for bacterial targeting and drug delivery. For instance, the Gram-positive pathogen *S. aureus* utilizes two siderophores, staphyloferrin A and staphyloferrin B (**69**, Figure 12A).[110] Enterobactin (**71**, Figure 12B) is a siderophore produced by multiple Gram-negative pathogens, including *E. coli* and *S. typhimurium*.[111] *P. aeruginosa* and other pathogens have effectively developed receptors to recognize and transport iron(III)-siderophore complexes from other bacterial species (xenosiderophores) providing a competitive growth advantage. Although

enterobactin is not produced by *P. aeruginosa*, this siderophore can promote iron uptake in this pathogen.[111]

These iron-specific uptake systems have provided a promising platform for targeted antibiotic delivery to select pathogens, especially for Gram-negative pathogens that present challenges regarding compound penetration as a result of two cellular membranes. Miller and co-workers have pioneered this area with much success in recent years with several inspiring examples of potent and targeted antibiotic delivery using a “Trojan horse” strategy that links antibiotics to various synthetic siderophores (sideromycins).[111–118] One example is presented in Figure 12C, where Miller and colleagues designed triscatecholate sideromycin **73**, inspired by catechol-based siderophore enterobactin **71**, which is utilized to target *P. aeruginosa*.[111] Sideromycin **73** was designed to have a linker moiety for attaching an antibiotic agent, in this case amoxicillin (ampicillin was also attached, not shown) to afford “Trojan horse” conjugate **74** (note: acetate groups were installed on catechol moieties to prevent pharmacological side effects and serve as prodrugs while circumventing potential methylation via a catechol *O*-methyl-transferase that would result in the loss of iron binding capabilities of the siderophore). Trojan horse conjugate **74** demonstrated potent antibacterial activities against *P. aeruginosa* strains in iron-deficient media, which resulted from the hijacking of energy-dependent active bacterial iron uptake systems required for bacterial growth under these conditions.[111] During these studies, MIC values for **74** ranged from 0.05 to 0.39 μM under iron-deficient media compared to MIC values that ranged from 12.5 to 50 μM in iron-rich media (note: amoxicillin was inactive against these *P. aeruginosa* strains, MIC > 100 μM).

A more detailed schematic of the Trojan horse strategy to target Gram-negative pathogens can be found in Figure 13A. Recently, Miller’s group has published two outstanding examples of Trojan horse conjugates hijacking iron uptake systems that enable Gram-positive antibiotics (an oxazolidinone[117] and daptomycin;[116] Figure 13B and Figure 13C) to effectively target Gram-negative pathogens, including *Acinetobacter baumannii*. These impressive examples of Trojan horse antibiotic delivery also showcase “releasable linkers” versus “nonreleasable linkers” that are an important design component in these systems.

Oxazolidinones target bacterial ribosomes and are effective at treating Gram-positive infections; however, these agents are inactive against most Gram-negative pathogens as they are unable to penetrate their outer membrane, or if they do permeate the Gram-negative bacteria, they are rapidly effluxed.[117] This spectrum of activity along with these resistance mechanisms (lack of penetration, efflux) makes oxazolidinones ideal candidates for Trojan horse conjugation. With that, sideromycin **75** was designed as a dual active agent containing siderophore–cephalosporin–oxazolidinone components, which combine the Trojan horse entry of Gram-negative pathogens with β-lactamase triggered release upon destructive ring-opening of the cephalosporin moiety to liberate an active oxazolidinone (**76**; Figure 13B).[117]

In the arsenal of Trojan horse conjugate linkers, it is important to have releasable linker options to avoid conjugate structures that perturb critical drug–target interactions, ultimately preventing antibiotic activities. Early attempts to develop releasable linkers included functional groups that were hydrolyzable (i.e., ester cleavage by esterases[112]) or reductively

cyclized (i.e., trimethyl lock bioreductive activation,[115] not shown) and led to problems with premature antibiotic release before iron-uptake dependent penetration of Gram-negative bacteria.[117] The cephalosporin linker in **75** requires the enzymatic activity of intracellular β-lactamases for "suicide" antibiotic release, bypassing premature release issues presented by other releasable linker systems. In initial proof-of-concept experiments, **75** underwent rapid and complete hydrolysis by purified ADC-1 β-lactamases, which are ADC enzymes found in *A. baumannii* that are capable of hydrolyzing cephalosporin antibiotics.[117]

The siderophore–cephalosporin–oxazolidinone **75** demonstrated impressive antibacterial activities against multiple Gram-negative pathogens, including *A. baumannii* (multiple, drug-resistant isolates; MIC = 0.4–6.25 μM), *E. coli* (MIC < 0.025 μM), and *P. aeruginosa* (MIC = 0.2–0.4 μM).[117] The corresponding oxazolidinone **76**, alone or when linked directly to the siderophore moiety (without cephalosporin to release **76**), was inactive against these pathogens (MIC from >50 to >500 μM). Interestingly, the siderophore–cephalosporin moiety alone (without oxazolidinone **76**; structure not shown) has moderate to good activities against some pathogens but is dramatically enhanced with all three moieties (**75**) intact against *A. baumannii*. For instance, against *A. baumannii* ATCC BAA 1800, the siderophore-cephalosporin components report MIC = 25 μM versus MIC = 0.8 μM for siderophore–cephalosporin–oxazolidinone **75**, demonstrating a clear structure–activity relationship for the necessity of all three structural components to display potent antibacterial activities at a level that is clinically relevant.

In separate work, Miller and co-workers coupled a mixed synthetic ligand analogue of *A. baumannii* siderophore fimsbactin with daptomycin to give conjugate **79**.[116] Daptomycin is a large, negatively charged lipopeptide anti-biotic that has significant value as a therapeutic agent against Gram-positive pathogens only. Although daptomycin's mechanism is not fully understood, it has been found to bind and disrupt bacterial cell membranes, resulting in rapid depolarization, concomitant ion efflux and dysregulation of nucleic acid and protein synthesis, and subsequent bactericidal death.[119] Prior structure–activity relationship investigations revealed that acylation of the primary amine of the ornithine residue in daptomycin was well-tolerated, and thus the Miller group used this information in the design of daptomycin-siderophore conjugate **79**.[116] Regarding chemical synthesis, the trichloroethyl chloroformate (Troc) protecting group of **77** was removed using zinc in the presence of glutaric anhydride to afford **78** as a benzyl protected siderophore bearing a (nonreleasable) glutarate linker for subsequent conjugation (Figure 14). A mixed anhydride of **78** was generated in situ before subjecting the siderophore-linker moiety to daptomycin under aqueous reaction conditions for conjugation via amide bond formation. Final hydrogenolytic removal of the benzyl groups provided target daptomycin-siderophore conjugate **79**.[116]

Siderophore-daptomycin conjugate **79** was shown to bind iron(III) stoichiometrically and demonstrated profound effectiveness against *A. baumannii* strains (MIC = 0.4–0.8 μM).[116] As predicted, daptomycin itself was inactive against *A. baumannii* strains (MIC > 100 μM) when tested alongside conjugate **79**. To demonstrate the importance of iron-binding and uptake regarding conjugate **79**, its synthetic precursor bearing bis benzyl group protected catechol moieties (structure not shown) proved to be completely inactive against *A.*

baumannii (MIC > 50 μM). When tested against other Gram-negative pathogens, such as *P. aeruginosa*, *Burkholderia multivorans*, and *Escherichia coli*, conjugate **79** proved to be inactive (MIC > 100 μM), demonstrating the selective targeting of this Trojan horse conjugate toward *A. baumannii*.

Following in vitro assessment, Trojan horse conjugate **79** was advanced to testing in mice.[116] Intravenous administration of **79** at 250 mg/kg in ICR mice resulted in no observed adverse effects. Following favorable toxicity studies in mice, conjugate **79** was evaluated for in vivo efficacy in a sepsis model of infection in female ICR mice using *A. baumannii* 17961. Mice were infected with *A. baumannii* via intraperitoneal (ip) administration, and treatments with conjugate **79** (5, 10, 25 mg/kg) were provided intravenously (iv) 30 min and 24.5 h after infection. In this study, all six mice that did not receive treatment with **79** died after 1 day; however, mice treated with **79** at 10 and 25 mg/kg resulted in survival in 4 of 5 mice (at each test concentration) while only 1 of 5 mice survived with **79** at 5 mg/kg, demonstrating a dose-dependent in vivo efficacy against *A. baumannii*. This is an outstanding demonstration of the clinical applications that the Trojan horse strategy can be utilized to target Gram-negative pathogens in human patients.

Cefiderocol (S-649266; structure not shown) is a catechol-bearing siderophore–cephalosporin conjugate that demonstrates potent antibacterial activities against a broad range of Gram-negative pathogens (e.g., carbepenem-resistant *Enterobacteriaceae*, *P. aeruginosa, A. baumannii*).[120] Cefiderocol has been advanced to clinical studies in human patients, demonstrating the translational potential of the Trojan horse strategy. In a clinical trial for the treatment of complicated urinary tract infection with antibiotic-resistant Gram-negative pathogens, cefiderocol was shown to be noninferior when compared to imipenem–cilastatin treated patients.[121] Currently, cefiderocol is being investigated in clinical trials for hospital-acquired pneumonia and carbapenem-resistant infections. Collectively, this body of work aimed at targeting iron uptake mechanisms in bacteria to deliver antibiotics in a Trojan horse fashion is a promising approach to overcome antibiotic-resistant infections.

ClpP PROTEASE-ACTIVATING AGENT ADEP4 FOR PERSISTER CELL AND BIOFILM ERADICATION

Isolated from *Strepomyces hawaiiensis*, the acyldepsipeptides (ADEPs) are a class of natural product antibiotics that have been shown to exhibit potent activities against Gram-positive bacteria including methicillin-resistant *Staphylococcus aureus* (MRSA) and vancomycin-resistant *Enterococci*.[122,123] The antibacterial activities for the natural product ADEP1 (**80**, Figure 15) and related synthetic analogues were evaluated by Brötz-Oesterhelt and co-workers, wherein ADEP1 reported a 8.76 μM IC_{50} value against MRSA. In addition, synthetic analogues ADEP2 (**81**) and ADEP4 (**82**) also reported therein demonstrated markedly improved activity (500 nM and 64.9 nM, respectively).[124] Furthermore, ADEP1 and ADEP4 were efficacious in vivo against both *S. aureus* and *E. faecalis* infection models. ADEP4 demonstrated the ability to rescue 80% of mice from mortal *S. aureus* infections following a single dose of 12.5 mg/kg. The group used genomic analyses to identify the

target for ADEP analogues as ClpP (caseinolytic protease), a highly conserved, cylindrical bacterial peptidase.[124]

The ClpP serine peptidase employs an energy-dependent process implicated in biological functions such as protein quality control, degradation of transient regulatory proteins, and clearance of cellular debris following conditions of bacterial stress.[125,126] Under normal homeostatic conditions, ClpP binds to ATP-dependent cochaperones (e.g., ATPases) which help regulate the unfolding and translocation of proteins into the proteolytic sites of ClpP. Crystal structures of ADEP1 (**80**) bound to *Escherichia coli* ClpP showed that ADEP analogues occupy the site of ATPase binding.[127] The ClpP–ADEP interaction promotes the conversion of the ClpP entrance pore from a closed-to an open-gate form (Figure 16). This allosteric control of the ClpP barrel conformation bypasses the need for an associated cochaperone (an energy dependent process) and permits the unregulated entrance of proteins into the proteolytic active site.[128] The resultant increase of ClpP activity diverts proteolysis from native physiological proteins to nascent peptides, leading to inhibition of bacterial cell division.

In a departure from prior studies (evaluating ADEP-promoted protein degradation against rapidly dividing cells), Lewis and co-workers utilized proteomic analysis to demonstrate that stationary phase MRSA exposed to ADEP4 (**82**) resulted in a reduced abundance of 24% of cellular proteins compared to the untreated control.[129] Since stationary phase populations of *S. aureus* are typically nondividing (and thus notoriously difficult to treat), this finding unveiled a potential therapeutic intervention against dormant persister cells. To evaluate the effect of ADEP4 against dormant bacteria, a population of persister cells was treated with the agent and it was found that ADEP4 was capable of eradicating persister cells to the limit of detection. Conversely, rifampicin reported no effect on persister cell viability.

ADEP4 also reported remarkable killing of stationary phase *S. aureus* following 2 days of treatment, demonstrating a 4 log reduction of viable bacterial cell counts.[129] Since ClpP is a nonessential protein for *S. aureus*, the null *clpP* (the gene encoding the ClpP protease) mutation frequency is high ($\sim 10^{-6}$), and thus, rebounding populations were observed after day 3 of the experiments. It was surmised that formation of resistant mutants could be suppressed via coadministration of ADEP4 with conventional antibiotics. This co-treatment strategy eradicated persister cells to the limit of detection with no concomitant population rebound. It was found that although treatment of a *clpP* mutant strain with rifampicin demonstrated similar MIC values as that seen against of the wild-type strain, the mutant strains were less capable of producing persister cells (by an order of 10-to 100-fold). The conclusion was that *clpP* mutations (e.g., those resulting from ADEP treatment) may render the bacteria less fit and thus more susceptible to other antibiotics.

By use of 96-well plate, non-Calgary Biofilm Device assays, the ability of the ADEP4–rifampicin combination to eradicate bacterial biofilms was also evaluated.[129] Following a 24-h *S. aureus* UAMS-1 biofilm establishment, wells were treated with the ADEP4–rifampicin combination (6.49 μM ADEP4, 10 × MIC; 0.49 μM rifampicin, 10 × MIC), resulting in eradicated biofilms (>4 log-fold reduction) following 3 days of treatment. The ADEP4–rifampicin combination was also shown to be highly efficacious in deep-seated in

vivo infection models. Following a 24 h infection period, histopathology was used to confirm the adherence of bacterial biofilms to mouse thigh muscle tissue. Treatment of the infection with the ADEP4–rifampicin combination resulted in an eradication of the biofilm-associated infection within 24 h (representing a >4 log-fold reduction). In contrast, rifampicin, vancomycin, or a combination of both could not eradicate the infection although decreased viable cell counts were observed.

The LaFleur group was also able to show that the ADEP–antibiotic combination strategy could be expanded to include additional clinically used antibiotics.[130] LeFleur and co-workers reported ADEP4 activity against stationary phase multidrug-resistant *E. faecalis* V583 when treated in combination with ampicillin, ciprofloxacin, daptomycin, oritavancin, or tigecycline. In these cases, the ADEP4–antibiotic combination yielded a 5 log reduction in bacterial cell survival. This was especially interesting as the activity was observed regardless of the mechanistic class of partnered antibiotic. Expression and purification of *E. faecium* ClpP permitted the use of a fluorometric monitoring assay used to evaluate casein degradation wherein it was reported that ADEP4 activated ClpP with an EC_{50} of 0.53 μM. A crystal structure was also disclosed, highlighting the binding of ADEP4 to the hydrophobic pockets located between subunits at the apical and distal ends of ClpP. In a murine model of peritoneal septicemia, treatment with ADEP4 (50 mg/kg) and ampicillin (50 mg/kg) yielded a 2 $\log_{10}$ greater reduction in average bacterial burden when compared to antibiotic monotherapy and a 4 $\log_{10}$ reduction of viable bacterial cells relative to the vehicle control.

Encouraged by the in vivo antibacterial efficacy of ADEP analogues, several groups have put forth medicinal chemistry efforts to improve on this therapeutic strategy. In an attempt to reduce entropic binding penalties, Sello and co-workers disclosed an enhancement of ADEP analogues via introduction of conformational restriction.[131] This strategy was realized via replacement of key macrocyclic residues. The result of the rigidified ADEP analogues was a 20-fold improvement of in vitro *S. aureus* activity from MIC = 649 nM [129] for ADEP4 compared to 30.6 nM for ADEP1g (**83**). Building upon the library of known antibacterial ADEP analogues, the Duerfeldt group described an attempt to remedy a potential metabolic liability of the ADEP series (i.e., the readily hydrolyzed ester within the lactone core).[132] On the basis of the reported crystal structures of ADEPs bound to ClpP, it seemed evident that replacement of the ester with an amide may have no influence on the interaction of the ADEPs with ClpP. Alas, Duerfeldt and co-workers were surprised to learn that amide-containing ADEP analogues **85** and **86** were markedly less active (by up to 100-fold) than the corresponding ester ADEP analogue **84**. It was surmised that although the ester oxygen may not participate in molecular interactions with the target, its replacement with an amide nitrogen disrupts intramolecular hydrogen bonds (**87**, Figure 15) and thus compromises the compact conformation of the active agent (which presumably assists in membrane permeability). Although no biofilm eradication or in vivo assays were conducted as part of these recent studies, the reported novel agents demonstrate that the ADEP-based therapeutic approaches are fruitful pursuits and initial efforts to advance these agents toward clinical use have been very promising.

HALOGENATED PHENAZINE BIOFILM-ERADICATING AGENTS

Cystic fibrosis (CF) patients are plagued with chronic lung infections, which became a source of chemical inspiration for our lab to identify new biofilm-eradicating agents. Many young CF patients are known to experience initial *S. aureus* lung infections.[133] As these patients age, *P. aeruginosa* subsequently co-infects the lung and is believed to eradicate *S. aureus* using a series of phenazine antibiotics, including pyocyanin.[133–137] We believe that the initial *S. aureus* infections establish surface-attached biofilms on the inside of lung tissues as CF patients have lung infections that span multiple years.

In our initial work, we synthesized a diverse series of 13 phenazine compounds, including five naturally occurring phenazines.[138] With literature reports of pyocyanin as the main antibiotic of this class responsible for activities against *S. aureus*, we were sure to include this compound in our initial screening collection. Interestingly, in our initial antibacterial screens against *S. aureus* and *S. epidermidis*, we found that 2-bromo-1-hydroxyphenazine, a marine *Streptomyces* derived phenazine, demonstrated good antibacterial activities with MIC values of 6.25 μM against these pathogens (pyocyanin reported MICs of 50 μM).[138] In addition, we found that related synthetic analogue 2,4-dibromo-1-hydroxyphenazine (not shown) demonstrated improved antibacterial activities against *S. aureus* and *S. epidermidis* with MICs of 1.56 μM. In later work, we found that 2,4-dibromo-1-hydroxyphenazine was able to eradicate methicillin-resistant *Staphylococcus aureus* biofilms and reported a minimum biofilm eradication concentration, or MBEC, of ~100 μM (note: when tested alongside 2,4-dibromo-1-hydroxyphenazine, vancomycin reported an MBEC of >2000 μM in Calgary Biofilm Device assays despite an MBEC of 4 μM against planktonic cells in the same experiment, demonstrating a significant level of biofilm tolerance toward vancomycin).[139]

After demonstrating that 2,4-dibromo-1-hydroxyphenazine eradicates MRSA biofilms, we worked to develop modular, convergent synthetic routes to new “halogenated phenazine” (HP; Figure 17A, see structure **95**) small molecules.[140–143] Chemical synthesis pathways involving phenylenediamine (**88**) condensation with quinone **89**,[140,141] a Wohl–Aue reaction[142] (aniline **90** condensed with 2-nitroanisole **91**), and a Buchwald–Hartwig cross-coupling/reductive cyclization path-way[143] (fusing aniline **92** with 2-bromo-3-nitroanisole **93**) enabled rapid access to a diversity of 1-methoxyphenazines (**94**) with various substitutions at the 6–9 positions of the HP scaffold (**95**). A final boron tribromide (BBr_3) demethylation and *N*-bromosuccinimide (NBS) bromination sequence afforded target HPs 95. These synthetic efforts and subsequent antibacterial studies have led to the identification of several highly potent biofilm-eradicating agents, including HPs **96**–**98**, which demonstrate up to 50-fold more potent biofilm killing activities in Calgary Biofilm Device assays compared to parent 2,4-dibromo-1-hydroxyphenazine (e.g., **98** reported an MBEC of 2.35 μM against MRSA biofilms[143]).

These efforts have enabled a detailed structure–activity relationship understanding regarding halogenated phenazine antibacterial agents (see **99**, Figure 17B).[138–143] In general, substitution at the 6- and 7-positions of the HP scaffold is typically well-tolerated and enhances antibacterial activities compared to the corresponding unsubstituted HP; however,

the 8-position of the HP scaffold can influence antibacterial potency in a positive (e.g., halogens improve activity) or negative (e.g., methyl reduces activity) fashion. Interestingly, we found that substitution at the 9-position of the HP scaffold completely abolishes all antibacterial activities. We later discovered the reason for a loss in activity regarding 9-substituted HPs after learning that active HP compounds bind metal(II) cations between the hydroxyl oxygen and adjacent nitrogen (forming a five-membered chelate upon metal binding), which plays a critical role in the antibacterial mode of action. Substituents at the 9-position of the HP scaffold, including a relatively small methyl group, impede the critical metal-chelation event for antibacterial activities.[140] Interestingly, general metal-chelating agents (EDTA and TPEN) have been tested alongside HPs and are unable to eradicate bacterial biofilms, highlighting the unique metal-dependent mechanism behind HP small molecules.[141–143]

In ongoing efforts to translate HP biofilm-eradicating agents for clinical applications, we are using the SAR knowledge of the HP scaffold to pursue multiple prodrug strategies to functionalize the phenolic hydroxyl group to abolish metal-chelation until selective release within bacterial cells.[142,143] This approach provides a platform for extensive developments, including (1) tuning of physicochemical properties (e.g., installation of PEG group to increase water solubility[142,143]) and (2) diverse functional triggers for HP release (e.g., bioreduction of the quinone in **101** is required to liberate the corresponding HP agent[143]). Despite initial success with HPs **100** and **101**, continued prodrug efforts are ongoing with the goal of developing an effective clinical agent for biofilm infections.

In separate work, we used HP-14 (**96**, MBEC = 6.25 μM) as a probe molecule for transcriptomic analysis of treated and untreated MRSA biofilms using RNA-seq technology.[144] This platform allowed us to define new cellular targets and pathways critical to biofilm survival, which is challenging to study as these surface-attached bacterial communities are composed of slow-growing or nonreplicating cells. Treating an established MRSA biofilm with HP-14 at low concentration (0.625 μM; 1/ 10 MBEC) for 20 h enabled the identification of >200 gene transcripts that were either up- or down-regulated (≥2.0-fold change in gene expression) compared to vehicle control.

Using a WoPPER gene cluster analysis tool, we identified 37 gene clusters with alterations in MRSA biofilm gene expression profiles following 20 h treatment with HP-14.[144] Upon exposure of HP-14 to MRSA biofilms, six gene clusters involved in iron acquisition were found to be dramatically up-regulated (“activated”) via WoPPER analysis, including: *hts*/*sfa* (staphyloferrin A; siderophore), *sir*/*sbn* (staphyloferrin B), *isd* (iron-regulated surface determinant; heme iron acquisition), MW0695 (hypothetical protein, similar to ferrichrome ABC transporters), and *f hu* (ferric hydroxamate uptake; two gene clusters). Following validation of these results using RT-qPCR experiments, a time-course assessment of MRSA biofilms treated with HP-14 (0.625 μM; 1/10 MBEC) revealed that four iron acquisition gene clusters (*isd*, *sbn*, *sfa*, MW0695) were activated in 1 h. The rapid activation of multiple iron uptake gene clusters by low concentrations of HP-14 is profound, as bacterial biofilms are notorious for their dormant phenotypes. Following 4 and 8 h of HP-14 exposure at 0.625 μM (1/10 MBEC), MRSA biofilms demonstrated more significant activation levels of these iron uptake genes (e.g., *isdB*, 22.3-fold activation after 4 h). Interestingly, EDTA and TPEN

(5 μM; general metal-chelating agents) were unable to activate iron acquisition genes in MRSA biofilms,[144] which aligns with our previous observations that these metal-chelating agents are unable to eradicate MRSA biofilms (MBEC of >2000 μM) in Calgary Biofilm Device assays.[141–143]

On the basis of RNA-seq findings, we believe HP-14 induces rapid iron starvation in MRSA biofilms, which leads to eradication of these surface-attached bacteria.[144] With the lipophilic properties of HP-14 (cLogP = 6.25) combined with potent MRSA biofilm eradication activity (MBEC = 6.25 μM), an iron chelating moiety, and rapid activation of multiple iron uptake gene clusters, we believe that this HP rapidly diffuses into biofilm cells and binds iron(II) following the intracellular release of iron(II) from a siderophore or heme. A proposed scheme of HP-14 inducing iron starvation and MRSA biofilm eradication is presented in Figure 18 and aligns with our WoPPER gene cluster analysis and subsequent RT-qPCR results in time-course studies. In addition, we believe that EDTA and TPEN are not able to efficiently penetrate biofilm cells, which is why they are unable to activate iron uptake genes or eradicate biofilms when tested alongside active HP biofilm-eradicating agents. This work not only demonstrates HP-14's ability to rapidly induce iron starvation in MRSA biofilms but highlights an impressive level of sensitivity along with rapid response rates of bacterial biofilms to small molecule threats. In addition, these findings suggest that iron starvation of surface-attached bacterial communities could serve as the Achilles heel to persistent and recurring biofilm infections in the clinic.

CONCLUSIONS

Despite increasing concerns regarding antibiotic resistance, antibiotic drug discovery is entering a dynamic and exciting new era. The multidisciplinary approaches of the research programs presented here have, in part, contributed to the reinvigoration of natural-product-based research for antibiotic discovery. Other impactful programs inspired by natural products, yet not included in this Perspectives article, include Genentech's optimized arylomycin analogues for Gram-negative pathogens[145] and Boger et al.'s vancomycin work.[146–150] The classic tools of synthetic chemistry, microbiology, and chemical biology have been applied in novel ways to answer questions about bacterial pathogenesis and to design innovative therapeutic approaches for combatting infections. Significant challenges lie ahead, but these research efforts along with others have helped pave the way for critical and desperately needed discoveries to address problems presented by antibiotic resistance and tolerance.

ACKNOWLEDGMENTS

We acknowledge the National Institute of General Medical Sciences of the National Institutes of Health for providing financial support (Grant R35GM128621 to R.W.H.). A.T.G. and G.M.B. were each awarded University of Florida Graduate School Fellowships. A.C.-R. is supported by a postdoctoral fellowship from CONACYT (CVU Grant 346860).

Biographies

Yasmeen Abouelhassan received a Ph.D. in Medicinal Chemistry with Prof. Robert W. Huigens at the University of Florida in 2018. She received her B.S. in Pharmaceutical

Sciences from Cairo University, Egypt, in 2012. Her Ph.D. research focused on the identification of novel biofilm-eradicating agents against Gram-positive bacteria. This research led to the discovery of phenazine antibiotic derivatives as potent methicillin-resistant *S. aureus* biofilm eradicators operating through a novel iron starvation mechanism.

Aaron T. Garrison received his Ph.D. in Medicinal Chemistry under Professor Robert W. Huigens III at the University of Florida in 2017 where he synthesized potent halogenated phenazine and quinoline small molecules, including diverse prodrug analogues of lead compounds. Thereafter, he accepted a postdoctoral position with Professor Craig W. Lindsley at the Vanderbilt Center for Neuro-science Drug Discovery. His research is presently focused on the design and synthesis of negative allosteric modulators of the muscarinic acetylcholine receptor subtype 5 (M_5) for the treatment of opioid and ethanol dependence. His additional research projects include the development of synthetic methodology to facilitate the discovery of novel therapeutics.

Hongfen Yang received a B.S. in Chemistry from Hubei University in Wuhan, China. She then moved to the University of Chinese Academy of Sciences in Beijing under the guidance of Professor Wu, where she obtained a M.S. in Bioinorganic Chemistry. Currently, Hongfen is a fourth year graduate student in the Medicinal Chemistry Department at the University of Florida under the supervision of Professor Huigens. Her doctoral research involves the design, chemical synthesis, and biological evaluation of new halogenated phenazine biofilm-eradicating agents.

Alejandra Chávez-Riveros obtained her M.S. and Ph.D. in Chemical Sciences from the National Autonomous University of Mexico (Universidad Nacional Autónoma de México, UNAM). Her doctoral work focused on the design and synthesis of steroidal 5α-reductase inhibitors under the mentorship of Professor Eugene Bratoeff. She went to Evestra Inc. for a predoctoral internship, where she synthesized antiprogestins. Upon graduation with a Ph.D. in 2016, she joined Professor Luis D. Miranda's group at the Institute of Chemistry UNAM for postdoctoral studies and developed the synthesis of novel macrocycles, which demonstrate anti-inflammatory activities. She is currently a Postdoctoral Research Associate in Professor Huigens' lab at the University of Florida in the Department of Medicinal Chemistry, where she is developing new synthetic methodologies for ring distortion of indole alkaloids.

Gena M. Burch is the Kenneth F. Finger Memorial Fellow in the Infectious Disease and Pharmacokinetics Laboratory at the University of Florida. She received a PharmD in 2016, followed by a M.S. in Medicinal Chemistry in 2018 from the University of Florida under the supervision of Dr. Robert W. Huigens III working on the discovery and development of novel antibacterial and biofilm-eradicating agents. Her current research includes liquid chromatography–tandem mass spectrometry method development for the determination of serum concentrations for antimicrobial drugs. Her clinical research efforts are focused on therapeutic drug monitoring and clinical pharmacokinetics for patients with bacterial and mycobacterial infections.

Robert W. Huigens III received a Ph.D. in Chemistry with Professor Christian Melander at NC State University in 2009. He then moved to the University of Illinois of Urbana–Champaign as an American Cancer Society Postdoctoral Fellow under the guidance of Professor Paul Hergenrother. In 2013, Huigens began his independent career as an Assistant Professor of Medicinal Chemistry at the University of Florida. The Huigens lab has interdisciplinary drug discovery programs inspired by natural products that aim to (1) discover novel antibacterial agents that eradicate bacterial biofilms and (2) rapidly generate architecturally complex and diverse compound libraries from readily available indole alkaloids.

ABBREVIATIONS USED

Accum	accumulation
AcOH	acetic acid
ADEP	acyldepsipeptide (antibacterial agent)
AfBPP	affinity-based protein profiling
Asp	aspartic acid
aq	aqueous
BBr_3	boron tribromide
BINAP	2,2′-bis(diphenylphosphino)-1,1′-binaphthyl
Bn	benzyl
Boc	*tert*-butyloxycarbonyl
C	carbon
ClpP	caseinolytic protease
CF	cystic fibrosis
CFU	colony forming unit (viable bacterial count)
DHF	dihydrofolate
DIPEA	*N,N*-diisopropylethylamine
DMAP	4-dimethylaminopyridine
DMF	dimethylformamide
DMP	Dess-Martin periodinane
DMPU	*N,N′*-dimethylpropyleneurea
DNA	deoxyribonucleic acid

DNM	deoxynybomycin
EDC	1-ethyl-3-(3-dimethylaminopropyl)carbodiimide
EDTA	ethylenediaminetetraacetic acid
ETC	electron transport chain
EtOAc	ethyl acetate
FDA	Food and Drug Administration
Fe	iron
HATU	hexafluorophosphate azabenzotriazole tetramethyluranium
Glob	globularity
HF	hydrogen fluoride
HOAt	1-hydroxy-7-azabenzotriazole
HP	halogenated phenazine
Isd	heme-iron complex
KOH	potassium hydroxide
LCMS/MS	liquid chromatography-mass spectrometry
LDA	lithium diisopropylamide
LiOH	lithium hydroxide
Lys	lysine
MBEC	minimum biofilm eradication concentration
mg/kg	milligrams per kilogram
MIC	minimum inhibitory concentration (lowest concentration that demonstrates complete bacterial growth inhibition)
MRSA	methicillin-resistant *Staphylococcus aureus*
$NaBH_4$	sodium borohydride
NaHMDS	sodium bis(trimethylsilyl)amide
NaOEt	sodium ethoxide
NBS	*N*-bromosuccinimide
nmol	nanomole
NMR	nuclear magnetic resonance

NRPS	non-ribosomal peptide synthetase
PABA	*p*-aminobenzoate
Pd	palladium
Phe	phenylalanine
PhMe	toluene
rRNA	ribosomal ribonucleic acid
RB	rotatable bond (rigidity)
Ru	ruthenium
SAR	structure-activity relationship
sbn	staphyloferrin B
SdhC	succinate dehydrogenase C subunit
SEM	2-(trimethylsilyl)ethoxymethyl
Ser	serine
sfa	staphyloferrin A
TBAF	tetrabutylammonium fluoride
TBDPS	*tert*-butyldiphenylsilyl
TBS	*tert*-butyldimethylsilyl
TBSCl	*tert*-butyldimethylsilyl chloride
TCA	tricarboxylic acid
Tf	triflate
TFA	trifluoroacetic acid
THF	tetrahydrofolate
THF	tetrahydrofuran
Thr	threonine
TMEDA	tetramethylethylenediamine
TMS	trimethylsilyl
TPEN	*N,N,N′,N′*-tetrakis(2-pyridinylmethyl)-1,2-ethanediamine
Troc	trichloroethyl chloroformate
***μg*/mL**	micrograms per milliliter

μM	micromolar
VRE	vancomycin-resistant enterococci
WGS	whole genome sequencing
Zn	zinc

REFERENCES

(1). Lewis K Platforms for Antibiotic Discovery. Nat. Rev. Drug Discovery 2013, 12, 371–387. [PubMed: 23629505]

(2). Brown ED; Wright GD Antibacterial Drug Discovery in the Resistance Era. Nature 2016, 529, 336–343. [PubMed: 26791724]

(3). Blair JMA; Webber MA; Baylay AJ; Ogbolu DO; Piddock LJV Molecular Mechanisms of Antibiotic Resistance. Nat. Rev. Microbiol 2015, 13, 42–51. [PubMed: 25435309]

(4). Rossiter SE; Fletcher MH; Wuest WM Natural Products as Platforms To Overcome Antibiotic Resistance. Chem. Rev 2017, 117, 12415–12474. [PubMed: 28953368]

(5). Ali J; Rafiq QA; Ratcliffe E Antimicrobial Resistance Mechanisms and Potential Synthetic Treatments. Futur. Sci. OA 2018, 4, FSO290.

(6). Zaman SB; Hussain MA; Nye R; Mehta V; Mamun KT; Hossain N A Review on Antibiotic Resistance: Alarm Bells Are Ringing. Cureus 2017, 9, e1403. [PubMed: 28852600]

(7). Kohanski MA; Dwyer DJ; Collins JJ How Antibiotics Kill Bacteria: From Targets to Networks. Nat. Rev. Microbiol 2010, 8, 423–435. [PubMed: 20440275]

(8). Martinez JL General Principles of Antibiotic Resistance in Bacteria. Drug Discovery Today: Technol 2014, 11, 33–39.

(9). Wright GD Molecular Mechanisms of Antibiotic Resistance. Chem. Commun 2011, 47, 4055–4061.

(10). Garrison AT; Huigens RW Eradicating Bacterial Biofilms with Natural Products and Their Inspired Analogues That Operate Through Unique Mechanisms. Curr. Top. Med. Chem 2017, 17, 1954–1964.

(11). Lewis K Persister Cells, Dormancy and Infectious Disease. Nat. Rev. Microbiol 2007, 5, 48–56. [PubMed: 17143318]

(12). Lewis K Persister Cells. Annu. Rev. Microbiol 2010, 64, 357–372. [PubMed: 20528688]

(13). Marín M; Gudiol F Beta-Lactam Antibiotics. Enferm. Infecc. Microbiol. Clin 2003, 21, 42–55. [PubMed: 12550043]

(14). Hammes WP; Neuhaus FC On the Mechanism of Action of Vancomycin: Inhibition of Peptidoglycan Synthesis in Gaffkya Homari. Antimicrob. Agents Chemother 1974, 6, 722–728. [PubMed: 4451345]

(15). Chopra I; Roberts M Tetracycline Antibiotics: Mode of Action, Applications, Molecular Biology, and Epidemiology of Bacterial Resistance. Microbiol. Mol. Biol. Rev 2001, 65, 232–260. [PubMed: 11381101]

(16). Leclercq R Mechanisms of Resistance to Macrolides and Lincosamides: Nature of the Resistance Elements and Their Clinical Implications. Clin. Infect. Dis 2002, 34, 482–492. [PubMed: 11797175]

(17). Mingeot-Leclercq MP; Glupczynski Y; Tulkens PM Aminoglycosides: Activity and Resistance. Antimicrob. Agents Chemother 1999, 43, 727–737. [PubMed: 10103173]

(18). Weigelt J; Itani K; Stevens D; Lau W; Dryden M; Knirsch C; Linezolid CSSTI Study Group. Linezolid versus Vancomycin in Treatment of Complicated Skin and Soft Tissue Infections. Antimicrob. Agents Chemother 2005, 49, 2260–2266. [PubMed: 15917519]

(19). Maggi N; Pasqualucci CR; Ballotta R; Sensi P Rifampicin: A New Orally Active Rifamycin. Chemotherapy 2004, 11, 285–292.

(20). Wehrli W; Knüsel F; Schmid K; Staehelin M Interaction of Rifamycin with Bacterial RNA Polymerase. Proc. Natl. Acad. Sci. U. S. A 1968, 61, 667–673. [PubMed: 4879400]

(21). Nagaoka H; Kishi Y Further Synthetic Studies on Rifamycin S. Tetrahedron 1981, 37, 3873–3888.

(22). Palumbo M; Gatto B; Zagotto G; Palù G On the Mechanism of Action of Quinolone Drugs. Trends Microbiol 1993, 1, 232–235. [PubMed: 8137121]

(23). Blondeau JM Fluoroquinolones: Mechanism of Action, Classification, and Development of Resistance. Surv. Ophthalmol 2004, 49, S73–S78. [PubMed: 15028482]

(24). Bearden DT; Danziger LH Mechanism of Action of and Resistance to Quinolones. Pharmacotherapy 2001, 21, 224S–232S. [PubMed: 11642689]

(25). Fàbrega A; Madurga S; Giralt E; Vila J Mechanism of Action of and Resistance to Quinolones. Microb. Biotechnol 2009, 2, 40–61. [PubMed: 21261881]

(26). Bushby SRM; Hitchings GH Trimethoprim, A Sulphonamide Potentiator. Br. J. Pharmacol. Chemother 1968, 33, 72–90. [PubMed: 5301731]

(27). Sinha S; Shen X; Gallazzi F; Li Q; Zmijewski JW; Lancaster JR; Gates KS Generation of Reactive Oxygen Species Mediated by 1-Hydroxyphenazine, a Virulence Factor of *Pseudomonas aeruginosa*. Chem. Res. Toxicol 2015, 28, 175–181. [PubMed: 25590513]

(28). Davies J; Davies D Origins and Evolution of Antibiotic Resistance. Microbiol. Mol. Biol. Rev 2010, 74, 417–433. [PubMed: 20805405]

(29). Munita JM; Arias CA Mechanisms of Antibiotic Resistance. Microbiol. Spectrum 2016, 4, VMBF-0016–2015.

(30). Cassini A; Högberg LD; Plachouras D; Quattrocchi A; Hoxha A; Simonsen GS; Colomb-Cotinat M; Kretzschmar ME; Devleesschauwer B; Cecchini M; Ouakrim DA; Oliveira TC; Struelens MJ; Svetens C; Monnet DL; Burden of AMR Collaborative Group. Attributable Deaths and Disability-Adjusted Life-Years Caused by Infections with Antibiotic-Resistant Bacteria in the EU and the European Economic Area in 2015: A Population-Level Modelling Analysis. Lancet. Infect. Dis 2019, 19, 56–66. [PubMed: 30409683]

(31). Du D; Wang-Kan X; Neuberger A; van Veen HW; Pos KM; Piddock LJV; Luisi BF Multidrug Efflux Pumps: Structure, Function and Regulation. Nat. Rev. Microbiol 2018, 16, 523–539. [PubMed: 30002505]

(32). Delcour AH Outer Membrane Permeability and Antibiotic Resistance. Biochim. Biophys. Acta, Proteins Proteomics 2009, 1794, 808–816.

(33). Redgrave LS; Sutton SB; Webber MA; Piddock LJV Fluoroquinolone Resistance: Mechanisms, Impact on Bacteria, and Role in Evolutionary Success. Trends Microbiol 2014, 22, 438–445. [PubMed: 24842194]

(34). Pechère JC Macrolide Resistance Mechanisms in Gram-Positive Cocci. Int. J. Antimicrob. Agents 2001, 18 (Suppl. 1), 25–28.

(35). Wilson DN Ribosome-Targeting Antibiotics and Mechanisms of Bacterial Resistance. Nat. Rev. Microbiol 2014, 12, 35–48. [PubMed: 24336183]

(36). Brauner A; Fridman O; Gefen O; Balaban NQ Distinguishing Between Resistance, Tolerance and Persistence to Antibiotic Treatment. Nat. Rev. Microbiol 2016, 14, 320–330. [PubMed: 27080241]

(37). Miller MB; Bassler BL Quorum Sensing in Bacteria. Annu. Rev. Microbiol 2001, 55, 165–199. [PubMed: 11544353]

(38). Solano C; Echeverz M; Lasa I Biofilm Dispersion and Quorum Sensing. Curr. Opin. Microbiol 2014, 18, 96–104. [PubMed: 24657330]

(39). Defoirdt T; Brackman G; Coenye T Quorum Sensing Inhibitors: How Strong Is the Evidence? Trends Microbiol 2013, 21, 619–624. [PubMed: 24126008]

(40). Waters CM; Bassler BL Quorum Sensing: Cell-to-Cell Communication in Bacteria. Annu. Rev. Cell Dev. Biol 2005, 21, 319–346. [PubMed: 16212498]

(41). Worthington RJ; Richards JJ; Melander C Small Molecule Control of Bacterial Biofilms. Org. Biomol. Chem 2012, 10, 7457–7474. [PubMed: 22733439]

(42). Flemming H-C; Wingender J; Szewzyk U; Steinberg P; Rice SA; Kjelleberg S Biofilms: An Emergent Form of Bacterial Life. Nat. Rev. Microbiol 2016, 14, 563–575. [PubMed: 27510863]

(43). Bjarnsholt T The Role of Bacterial Biofilms in Chronic Infections. APMIS Suppl 2013, 121, 1–51.

(44). Donlan RM Biofilms: Microbial Life on Surfaces. Emerging Infect. Dis 2002, 8, 881–890. [PubMed: 12194761]

(45). Donlan RM; Costerton JW Biofilms: Survival Mechanisms of Clinically Relevant Microorganisms. Clin. Microbiol. Rev 2002, 15, 167–193. [PubMed: 11932229]

(46). Hall-Stoodley L; Costerton JW; Stoodley P Bacterial Biofilms: From the Natural Environment to Infectious Diseases. Nat. Rev. Microbiol 2004, 2, 95–108. [PubMed: 15040259]

(47). Lewis K; Shan Y Persister Awakening. Mol. Cell 2016, 63, 3–4. [PubMed: 27392143]

(48). Lewis K Persister Cells: Molecular Mechanism Related to Antibiotic Tolerance. Handb. Exp. Pharmacol 2012, 211, 121–133.

(49). Keren I; Kaldalu N; Spoering A; Wang Y; Lewis K Persister Cells and Tolerance to Antimicrobials. FEMS Microbiol. Lett 2004, 230, 13–18. [PubMed: 14734160]

(50). Wood TK Combatting Bacterial Persister Cells. Biotechnol. Bioeng 2016, 113, 476–483. [PubMed: 26264116]

(51). Defraine V; Fauvart M; Michiels J Fighting Bacterial Persistence: Current and Emerging Anti-Persister Strategies and Therapeutics. Drug Resist. Updates 2018, 38, 12–26.

(52). Stewart PS Mechanisms of Antibiotic Resistance in Bacterial Biofilms. Int. J. Med. Microbiol 2002, 292, 107–113. [PubMed: 12195733]

(53). Fux CA; Costerton JW; Stewart PS; Stoodley P Survival Strategies of Infectious Biofilms. Trends Microbiol 2005, 13, 34–40. [PubMed: 15639630]

(54). Ling LL; Schneider T; Peoples AJ; Spoering AL; Engels I; Conlon BP; Mueller A; Schäberle TF; Hughes DE; Epstein S; Jones M; Lazarides L; Steadman VA; Cohen DR; Felix CR; Fetterman KA; Millett WP; Nitti AG; Zullo AM; Chen C; Lewis K A New Antibiotic Kills Pathogens without Detectable Resistance. Nature 2015, 517, 455–459. [PubMed: 25561178]

(55). Nichols D; Cahoon N; Trakhtenberg EM; Pham L; Mehta A; Belanger A; Kanigan T; Lewis K; Epstein SS Use of Ichip for High-Throughput In Situ Cultivation of “Uncultivable” Microbial Species. Appl. Environ. Microbiol 2010, 76, 2445–2450. [PubMed: 20173072]

(56). Giltrap AM; Dowman LJ; Nagalingam G; Ochoa JL; Linington RG; Britton WJ; Payne RJ Total Synthesis of Teixobactin. Org. Lett 2016, 18, 2788–2791. [PubMed: 27191730]

(57). Jin K; Sam IH; Po KHL; Lin D; Ghazvini Zadeh EH; Chen S; Yuan Y; Li X Total Synthesis of Teixobactin. Nat. Commun 2016, 7, 12394. [PubMed: 27484680]

(58). Craig W; Chen J; Richardson D; Thorpe R; Yuan Y A Highly Stereoselective and Scalable Synthesis of L-allo-Enduracididine. Org. Lett 2015, 17, 4620–4623. [PubMed: 26356680]

(59). Jad YE; Acosta GA; Naicker T; Ramtahal M; El-Faham A; Govender T; Kruger HG; de la Torre BG; Albericio F Synthesis and Biological Evaluation of a Teixobactin Analogue. Org. Lett 2015, 17, 6182–6185. [PubMed: 26654835]

(60). Parmar A; Iyer A; Vincent CS; Van Lysebetten D; Prior SH; Madder A; Taylor EJ; Singh I Efficient Total Syntheses and Biological Activities of Two Teixobactin Analogues. Chem. Commun 2016, 52, 6060–6063.

(61). Parmar A; Iyer A; Lloyd DG; Vincent CS; Prior SH; Madder A; Taylor EJ; Singh I Synthesis of Potent Teixobactin Analogues against Methicillin-Resistant Staphylococcus aureus (MRSA) through the Replacement of L-*allo*-Enduracididine with Its Isosteres. Chem. Commun 2017, 53, 7788–7791.

(62). Parmar A; Iyer A; Prior SH; Lloyd DG; Goh ETL; Vincent CS; Palmai-Pallag T; Bachrati CZ; Breukink E; Madder A; Lakshminarayanan R; Taylor EJ; Singh I Teixobactin Analogues Reveal Enduracididine to be Non-essential for Highly Potent Antibacterial Activity and Lipid II Binding. Chem. Sci 2017, 8, 8183–8192. [PubMed: 29568465]

(63). Parmar A; Lakshminarayanan R; Iyer A; Mayandi V; Goh ETL; Lloyd DG; Chalasani MLS; Verma NK; Prior SH; Beurman RW; Madder A; Taylor EJ; Singh I Design and Synthesis of Highly Potent Teixobactin Analogues against *Staphylococcus aureus*, Methicillin-Resistant

Staphylococus aureus (MRSA), and Vancomycin-Resistant Enterococci (VRE) *In Vitro and In Vivo*. J. Med. Chem 2018, 61, 2009–2017. [PubMed: 29363971]

(64). Wu C; Pan Z; Yao G; Wang W; Fang L; Su W Synthesis and Structure–Activity Relationship Studies of Teixobactin Analogues. RSC Adv 2017, 7, 1923–1926.

(65). Zong Y; Sun X; Gao H; Meyer KJ; Lewis K; Rao Y Developing Equipotent Teixobactin Analogues against Drug-Resistant Bacteria and Discovering a Hydrophobic Interaction Between Lipid II and Teixobactin. J. Med. Chem 2018, 61, 3409–3421. [PubMed: 29629769]

(66). Jin K; Po KHL; Kong WY; Lo CH; Lo CW; Lam HY; Sirinimal A; Reuven JA; Chen S; Li X Synthesis and Antibacterial Studies of Teixtobactin Analogues with Non-Isostere Substitution of Enduracididine. Bioorg. Med. Chem 2018, 26, 1062–1068. [PubMed: 29398444]

(67). Ng V; Kuehne SA; Chan WC Rational Design and Synthesis of Modified Teixobactin Analogues: In Vitro Antibacterial Activity against Staphylococcus aurues, Propionibacterium acnes and Pseudomonas aeruginosa. Chem. - Eur. J 2018, 24, 9136–9147. [PubMed: 29741277]

(68). Richter MF; Drown BS; Riley AP; Garcia A; Shirai T; Svec RL; Hergenrother PJ Predictive Compound Accumulation Rules Yield a Broad-Spectrum Antibiotic. Nature 2017, 545, 299–304. [PubMed: 28489819]

(69). Fischbach MA; Walsh CT Antibiotics for Emerging Pathogens. Science 2009, 325, 1089–1093. [PubMed: 19713519]

(70). Payne DJ; Gwynn MN; Holmes DJ; Pompliano DL Drugs for Bad Bugs: Confronting the Challenges of Antibacterial Discovery. Nat. Rev. Drug Discovery 2007, 6, 29–40. [PubMed: 17159923]

(71). Nikaido H Molecular Basis of Bacterial Outer Membrane Permeability Revisited. Microbiol. Mol. Biol. Rev 2003, 67, 593–656. [PubMed: 14665678]

(72). Richter MF; Hergenrother PJ Broad-Spectrum Antibiotics, A Call for Chemists. Chem 2017, 3, 10–13.

(73). Richter MF; Hergenrother PJ The Challenge of Converting Gram-Positive-Only Compounds into Broad-Spectrum Antibiotics. Ann. N. Y. Acad. Sci 2019, 1435, 18–38. [PubMed: 29446459]

(74). Huigens RW; Morrison KC; Hicklin RW; Flood TA; Richter MF; Hergenrother PJ A Ring-Distortion Strategy to Construct Stereochemically Complex and Structurally Diverse Compounds from Natural Products. Nat. Chem 2013, 5, 195–202. [PubMed: 23422561]

(75). Hicklin RW; López Silva TL; Hergenrother PJ Synthesis of Bridged Oxafenestranes from Pleuromutilin. Angew. Chem., Int. Ed 2014, 53, 9880–9883.

(76). Rafferty RJ; Hicklin RW; Maloof KA; Hergenrother PJ Synthesis of Complex and Diverse Compounds through Ring Distortion of Abietic Acid. Angew. Chem., Int. Ed 2014, 53, 220–224.

(77). Garcia A; Drown BS; Hergenrother PJ Access to a Structurally Complex Compound Collection via Ring Distortion of the Alkaloid Sinomenine. Org. Lett 2016, 18, 4852–4855. [PubMed: 27650404]

(78). Tasker SZ; Cowfer AE; Hergenrother PJ Preparation of Structurally Diverse Compounds from the Natural Product Lycorine. Org. Lett 2018, 20, 5894–5898. [PubMed: 30204451]

(79). O'Shea R; Moser HE Physicochemical Properties of Antibacterial Compounds: Implications for Drug Discovery. J. Med. Chem 2008, 51, 2871–2878. [PubMed: 18260614]

(80). Parkinson EI; Bair JS; Nakamura B; Lee HY; Kuttab HI; Southgate EH; Lezmi S; Lau GW; Hergenrother PJ Deoxynybomycins Inhibit Mutant DNA Gyrase and Rescue Mice Infected with Fluoroquinolone-Resistant Bacteria. Nat. Commun 2015, 6, 6947. [PubMed: 25907309]

(81). Wright PM; Seiple IB; Myers AG The Evolving Role of Chemical Synthesis in Antibacterial Drug Discovery. Angew. Chem., Int. Ed 2014, 53, 8840–8869.

(82). Liu F; Myers AG Development of a Platform for the Discovery and Practical Synthesis of New Tetracycline Antibiotics. Curr. Opin. Chem. Biol 2016, 32, 48–57. [PubMed: 27043373]

(83). Charest MG; Lerner CD; Brubaker JD; Siegel DR; Myers AG A Convergent Enantioselective Route to Structurally Diverse 6-Deoxytetracycline Antibiotics. Science 2005, 308, 395–398. [PubMed: 15831754]

(84). Brubaker JD; Myers AG A Practical, Enantioselective Synthetic Route to a Key Precursor to the Tetracycline Antibiotics. Org. Lett 2007, 9, 3523–3525. [PubMed: 17691796]

(85). Sun C; Wang Q; Brubaker JD; Wright PM; Lerner CD; Noson K; Charest M; Siegel DR; Wang Y-M; Myers AG A Robust Platform for the Synthesis of New Tetracycline Antibiotics. J. Am. Chem. Soc 2008, 130, 17913–17927. [PubMed: 19053822]

(86). Wright PM; Myers AG Methodological Advances Permit the Stereocontrolled Construction of Diverse Fully Synthetic Tetracyclines Containing an All-Carbon Quaternary Center at Position C5a. Tetrahedron 2011, 67, 9853–9869. [PubMed: 22102762]

(87). Sun C; Hunt DK; Clark RB; Lofland D; O'Brien WJ; Plamondon L; Xiao X-Y Synthesis and Antibacterial Activity of Pentacyclines: A Novel Class of Tetracycline Analogs. J. Med. Chem 2011, 54, 3704–3731. [PubMed: 21500832]

(88). Clark RB; He M; Fyfe C; Lofland D; O'Brien WJ; Plamondon L; Sutcliffe JA; Xiao X-Y 8-Azatetracyclines: Synthesis and Evaluation of a Novel Class of Tetracycline Antibacterial Agents. J. Med. Chem 2011, 54, 1511–1528. [PubMed: 21302930]

(89). Zhang Z; Kitamura Y; Myers A An Efficient Directed Claisen Reaction Allows for Rapid Construction of 5,6-Disubstituted 1,3-Dioxin-4-Ones. Synthesis 2015, 47, 2709–2712.

(90). Seiple I; Hog D; Myers A Practical Protocols for the Preparation of Highly Enantioenriched Silyl Ethers of (R)-3-Hydroxypentan-2-one, Building Blocks for the Synthesis of Macrolide Antibiotics. Synlett 2015, 27, 57–60.

(91). Zhang Z; Fukuzaki T; Myers AG Synthesis of D-Desosamine and Analogs by Rapid Assembly of 3-Amino Sugars. Angew. Chem., Int. Ed 2016, 55, 523–527.

(92). Seiple IB; Zhang Z; Jakubec P; Langlois-Mercier A; Wright PM; Hog DT; Yabu K; Allu SR; Fukuzaki T; Carlsen PN; Kitamura Y; Zhou X; Condakes ML; SzczypiĔski FT; Green WD; Myers AG A Platform for the Discovery of New Macrolide Antibiotics. Nature 2016, 533, 338–345. [PubMed: 27193679]

(93). Hogan PC; Chen C-L; Mulvihill KM; Lawrence JF; Moorhead E; Rickmeier J; Myers AG Large-Scale Preparation of Key Building Blocks for the Manufacture of Fully Synthetic Macrolide Antibiotics. J. Antibiot 2018, 71, 318–325. [PubMed: 29018266]

(94). Tetraphase Pharmaceuticals Announces FDA Approval of XERAVA (Eravacycline) for Complicated Intra-Abdominal Infections (cIAI). Tetraphase Pharmaceuticals https://ir.tphase.com/news-releases/news-release-details/tetraphase-pharmaceuticals-announces-fda-approval-xeravatm (accessed Jan 21, 2019).

(95). Woodward RB; Logusch E; Nambiar KP; Sakan K; Ward DE; Au-Yeung BW; Balaram P; Browne LJ; Card PJ; Chen CH Asymmetric Total Synthesis of Erythromycin. 3. Total Synthesis of Erythromycin. J. Am. Chem. Soc 1981, 103, 3215–3217.

(96). Steele AD; Keohane CE; Knouse KW; Rossiter SE; Williams SJ; Wuest WM Diverted Total Synthesis of Promysalin Analogs Demonstrates That an Iron-Binding Motif Is Responsible for Its Narrow-Spectrum Antibacterial Activity. J. Am. Chem. Soc 2016, 138, 5833–5836. [PubMed: 27096543]

(97). Cox LM; Yamanishi S; Sohn J; Alekseyenko AV; Leung JM; Cho I; Kim SG; Li H; Gao Z; Mahana D; Zárate Rodriguez JG; Rogers AB; Robine N; Loke P; Blaser MJ Altering the Intestinal Microbiota During a Critical Developmental Window Has Lasting Metabolic Consequences. Cell 2014, 158, 705–721. [PubMed: 25126780]

(98). Gerber JS; Ross RK; Bryan M; Localio AR; Szymczak JE; Wasserman R; Barkman D; Odeniyi F; Conaboy K; Bell L; Zaoutis TE; Fiks AG Association of Broad- vs Narrow-Spectrum Antibiotics With Treatment Failure, Adverse Events, and Quality of Life in Children With Acute Respiratory Tract Infections. JAMA 2017, 318, 2325–2336. [PubMed: 29260224]

(99). Steele AD; Knouse KW; Keohane CE; Wuest WM Total Synthesis and Biological Investigation of (−)-Promysalin. J. Am. Chem. Soc 2015, 137, 7314–7317. [PubMed: 26024439]

(100). Knouse KW; Wuest WM The Enantioselective Synthesis and Biological Evaluation of Chimeric Promysalin Analogs Facilitated by Diverted Total Synthesis. J. Antibiot 2016, 69, 337–339. [PubMed: 26860469]

(101). Keohane CE; Steele AD; Fetzer C; Khowsathit J; Van Tyne D; Moynie L; Gilmore MS; Karanicolas J; Sieber SA; Wuest WM Promysalin Elicits Species-Selective Inhibition of Pseudomonas aeruginosa by Targeting Succinate Dehydrogenase. J. Am. Chem. Soc 2018, 140, 1774–1782. [PubMed: 29300464]

(102). Giglio KM; Keohane CE; Stodghill PV; Steele AD; Fetzer C; Sieber SA; Filiatrault MJ; Wuest WM Transcriptomic Profiling Suggests That Promysalin Alters the Metabolic Flux, Motility, and Iron Regulation in Pseudomonas putida KT2440. ACS Infect. Dis 2018, 4, 1179–1187. [PubMed: 29801413]

(103). Shapiro JA; Kaplan AR; Wuest WM From General to Specific: Can Pseudomonas Primary Metabolism Be Exploited for Narrow-Spectrum Antibiotics? ChemBioChem 2019, 20, 34–39. [PubMed: 30088315]

(104). Philippot L; Raaijmakers JM; Lemanceau P; van der Putten WH Going Back to the Roots: The Microbial Ecology of the Rhizosphere. Nat. Rev. Microbiol 2013, 11, 789–799. [PubMed: 24056930]

(105). Mendes R; Garbeva P; Raaijmakers JM The Rhizosphere Microbiome: Significance of Plant Beneficial, Plant Pathogenic, and Human Pathogenic Microorganisms. FEMS Microbiol. Rev 2013, 37, 634–663. [PubMed: 23790204]

(106). Li W; Estrada-de los Santos P; Matthijs S; Xie G-L; Busson R; Cornelis P; Rozenski J; De Mot R Promysalin, a Salicylate-Containing *Pseudomonas putida* Antibiotic, Promotes Surface Colonization and Selectively Targets Other *Pseudomonas*. Chem. Biol 2011, 18, 1320–1330. [PubMed: 22035801]

(107). Bilitewski U; Blodgett JAV; Duhme-Klair A-K; Dallavalle S; Laschat S; Routledge A; Schobert R Chemical and Biological Aspects of Nutritional Immunity-Perspectives for New Anti-Infectives that Target Iron Uptake Systems. Angew. Chem., Int. Ed 2017, 56, 14360–14382.

(108). Wilson BR; Bogdan AR; Miyazawa M; Hashimoto K; Tsuji Y Siderophores in Iron Metabolism: From Mechanism to Therapy Potential. Trends Mol. Med 2016, 22, 1077–1090. [PubMed: 27825668]

(109). Lyles KV; Eichenbaum Z From Host Heme To Iron: The Expanding Spectrum of Heme Degrading Enzymes Used by Pathogenic Bacteria. Front. Cell. Infect. Microbiol 2018, 8, 198. [PubMed: 29971218]

(110). Madsen JLH; Johnstone TC; Nolan EM Chemical Synthesis of Staphyloferrin B Affords Insight into the Molecular Structure, Iron Chelation, and Biological Activity of a Polycarboxylate Siderophore Deployed by the Human Pathogen *Staphylococcus aureus*. J. Am. Chem. Soc 2015, 137, 9117–9127. [PubMed: 26030732]

(111). Ji C; Miller PA; Miller MJ Iron Transport-Mediated Drug Delivery: Practical Syntheses and In Vitro Antibacterial Studies of Tris-Catecholate Siderophore-Aminopenicillin Conjugates Reveals Selectivity Potent Antipseudomonal Activity. J. Am. Chem. Soc 2012, 134, 9898–9901. [PubMed: 22656303]

(112). Ji C; Miller MJ Chemical Syntheses and *In Vitro* Antibacterial Activity of Two Desferrioxamine B-Ciprofloxacin Conjugates with Potential Esterase and Phosphatase Triggered Drug Release Linkers. Bioorg. Med. Chem 2012, 20, 3828–3836. [PubMed: 22608921]

(113). Wencewicz TA; Miller MJ Biscatecholate-Monohydrox-amate Mixed Ligand Siderophore-Carbacephalosporin Conjugates are Selective Sideromycin Antibiotics that Target *Acinetobacter baumannii*. J. Med. Chem 2013, 56, 4044–4052. [PubMed: 23614627]

(114). Wencewicz TA; Long TE; Möllmann U; Miller MJ Trihydroxamate Siderophore-Fluoroquinolone Conjugates Are Selective Sideromycin Antibiotics that Target *Staphylococcus aureus*. Bioconjugate Chem 2013, 24, 473–486.

(115). Ji C; Miller MJ Siderophore-Fluoroquinolone Conjugates Containing Potential Reduction-Triggered Linkers for Drug Release: Synthesis and Antibacterial Activity. BioMetals 2015, 28, 541–551. [PubMed: 25663417]

(116). Ghosh M; Miller PA; Möllmann U; Claypool WD; Schroeder VA; Wolter WR; Suckow M; Yu H; Li S; Huang W; Zajicek J; Miller MJ Targeted Antibiotic Delivery: Selective Siderophore Conjugation with Daptomycin Confers Potent Activity against Multidrug Resistant *Acinetobacter Baumannii* Both in Vitro and in Vivo. J. Med. Chem 2017, 60, 4577–4583. [PubMed: 28287735]

(117). Liu R; Miller PA; Vakulenko SB; Stewart NK; Boggess WC; Miller MJ A Synthetic Dual Drug Sideromycin Induces Gram-Negative Bacteria To Commit Suicide with a Gram-Positive Antibiotic. J. Med. Chem 2018, 61, 3845–3854. [PubMed: 29554424]

(118). Ghosh M; Lin Y-M; Miller PA; Möllmann U; Boggess WC; Miller MJ Siderophore Conjugates of Daptomycin are Potent Inhibitors of Carbapenem Resistant Strains of *Acinetobacter baumannii*. ACS Infect. Dis 2018, 4, 1529–1535. [PubMed: 30043609]

(119). Taylor SD; Palmer M The Action Mechanism of Daptomycin. Bioorg. Med. Chem 2016, 24, 6253–6268. [PubMed: 27288182]

(120). Ito A; Sato T; Ota M; Takemura M; Nishikawa T; Toba S; Kohira N; Miyagawa S; Ishibashi N; Matsumoto S; Nakamura R; Tsuji M; Yamano Y *In Vitro* Antibacterial Properties of Cefiderocol, a Novel Siderophore Cephalosporin, against Gram-Negative Bacteria. Antimicrob. Agents Chemother 2018, 62, e01454–17.

(121). Portsmouth S; van Veenhuyzen D; Echols R; Machida M; Ferreira JCA; Ariyasu M; Tenke P; Nagata TD Cefiderocol Versus Imipenem-Cilastatin for the Treatment of Complicated Urinary Tract Infections Caused by Gram-Negative Uropathogens: A Phase 2, Randomised, Double-Blind, Non-Inferiority Trial. Lancet Infect. Dis 2018, 18, 1319–1328. [PubMed: 30509675]

(122). Hinzen B; Raddatz S; Paulsen H; Lampe T; Schumacher A; Häbich D; Hellwig V; Benet-Buchholz J; Endermann R; Labischinski H; Brötz-Oesterhelt H Medicinal Chemistry Optimization of Acyldepsipeptides of the Enopeptin Class Antibiotics. ChemMedChem 2006, 1, 689–693. [PubMed: 16902918]

(123). Malik IT; Brötz-Oesterhelt H Conformational Control of the Bacterial Clp Protease by Natural Product Antibiotics. Nat. Prod. Rep 2017, 34, 815–831. [PubMed: 28375422]

(124). Brötz-Oesterhelt H; Beyer D; Kroll H-P; Endermann R; Ladel C; Schroeder W; Hinzen B; Raddatz S; Paulsen H; Henninger K; Bandow JE; Sahl H-G; Labischinski H Dysregulation of Bacterial Proteolytic Machinery by a New Class of Antibiotics. Nat. Med 2005, 11, 1082–1087. [PubMed: 16200071]

(125). Lee B-G; Park EY; Lee K-E; Jeon H; Sung KH; Paulsen H; Rübsamen-Schaeff H; Brötz-Oesterhelt H; Song HK Structures of ClpP in Complex with Acyldepsipeptide Antibiotics Reveal Its Activation Mechanism. Nat. Struct. Mol. Biol 2010, 17, 471–478. [PubMed: 20305655]

(126). Brötz-Oesterhelt H; Sass P Bacterial Caseinolytic Proteases as Novel Targets for Antibacterial Treatment. Int. J. Med. Microbiol 2014, 304, 23–30. [PubMed: 24119566]

(127). Li DHS; Chung YS; Gloyd M; Joseph E; Ghirlando R; Wright GD; Cheng YQ; Maurizi MR; Guarné A; Ortega J Acyldepsipeptide Antibiotics Induce the Formation of a Structured Axial Channel in ClpP: A Model for the ClpX/ClpA-Bound State of ClpP. Chem. Biol 2010, 17, 959–969. [PubMed: 20851345]

(128). Gersch M; Famulla K; Dahmen M; Göbl C; Malik I; Richter K; Korotkov VS; Sass P; Rübsamen-Schaeff H; Madl T; Brötz-Oesterhelt H; Sieber SA AAA+ Chaperones and Acyldepsipeptides Activate the ClpP Protease via Conformational Control. Nat. Commun 2015, 6, 6320. [PubMed: 25695750]

(129). Conlon BP; Nakayasu ES; Fleck LE; LaFleur MD; Isabella VM; Coleman K; Leonard SN; Smith RD; Adkins JN; Lewis K Activated ClpP Kills Persisters and Eradicates a Chronic Biofilm Infection. Nature 2013, 503, 365–370. [PubMed: 24226776]

(130). Brown Gandt A; Griffith EC; Lister IM; Billings LL; Han A; Tangallapally R; Zhao Y; Singh AP; Lee RE; LaFleur MD *In Vivo* and *In Vitro* Effects of a ClpP-Activating Antibiotic against Vancomycin-Resistant Enterococci. Antimicrob. Agents Chemother 2018, 62, e00424–18. [PubMed: 29784838]

(131). Carney DW; Schmitz KR; Truong JV; Sauer RT; Sello JK Restriction of the Conformational Dynamics of the Cyclic Acyldepsipeptide Antibiotics Improves Their Antibacterial Activity. J. Am. Chem. Soc 2014, 136, 1922–1929. [PubMed: 24422534]

(132). Li Y; Lavey NP; Coker JA; Knobbe JE; Truong DC; Yu H; Lin Y-S; Nimmo SL; Duerfeldt AS Consequences of Depsipeptide Substitution on the ClpP Activation Activity of Antibacterial Acyldepsipeptides. ACS Med. Chem. Lett 2017, 8, 1171–1176. [PubMed: 29152050]

(133). Machan ZA; Pitt TL; White W; Watson D; Taylor GW; Cole PJ; Wilson R Interaction Between *Pseudomonas aeruginosa* and *Staphylococcus aureus*: Description of an Antistaphylococcal Substance. J. Med. Microbiol 1991, 34, 213–217. [PubMed: 1902262]

(134). Laursen JB; Nielsen J Phenazine Natural Products: Biosynthesis, Synthetic Analogues, and Biological Activity. Chem. Rev 2004, 104, 1663–1685. [PubMed: 15008629]

(135). Price-Whelan A; Dietrich LEP; Newman DK Rethinking “Secondary” Metabolism: Physiological Roles for Phenazine Antibiotics. Nat. Chem. Biol 2006, 2, 71–78. [PubMed: 16421586]

(136). Dietrich LEP; Okegbe C; Price-Whelan A; Sakhtah H; Hunter RC; Newman DK Bacterial Community Morphogenesis Is Intimately Linked to the Intracellular Redox State. J. Bacteriol 2013, 195, 1371–1380. [PubMed: 23292774]

(137). Guttenberger N; Blankenfeldt W; Breinbauer R Recent Developments in the Isolation, Biological Function, Biosynthesis, and Synthesis of Phenazine Natural Products. Bioorg. Med. Chem 2017, 25, 6149–6166. [PubMed: 28094222]

(138). Borrero NV; Bai F; Perez C; Duong BQ; Rocca JR; Jin S; Huigens RW III. Phenazine Antibiotic Inspired Discovery of Potent Bromophenazine Antibacterial Agents against *Staphylococcus aureus* and *Staphylococcus epidermidis*. Org. Biomol. Chem 2014, 12, 881–886. [PubMed: 24389824]

(139). Garrison AT; Bai F; Abouelhassan Y; Paciaroni NG; Jin S; Huigens RW III. Bromophenazine Derivatives with Potent Inhibition, Dispersion and Eradication Activities against Staphylococcus aureus Biofilms. RSC Adv 2015, 5, 1120–1124.

(140). Garrison AT; Abouelhassan Y; Kallifidas D; Bai F; Ukhanova M; Mai V; Jin S; Luesch H; Huigens RW III. Halogenated Phenazines that Potently Eradicate Biofilms, MRSA Persister Cells in Non-Biofilm Cultures and *Mycobacterium tuber-culosis*. Angew. Chem., Int. Ed 2015, 54, 14819–14823.

(141). Garrison AT; Abouelhassan Y; Norwood VM IV; Kallifidas D; Bai F; Nguyen M; Rolfe M; Burch GM; Jin S; Luesch H; Huigens RW III. Structure-Activity Relationships of a Diverse Class of Halogenated Phenazines that Targets Persistent, Antibiotic-Tolerant Bacterial Biofilms and *Mycobacterium tuberculosis*. J. Med. Chem 2016, 59, 3808–3825. [PubMed: 27018907]

(142). Yang H; Abouelhassan Y; Burch GM; Kallifidas D; Huang G; Yousaf H; Jin S; Luesch H; Huigens RW III. A Highly Potent Class of Halogenated Phenazine Antibacterial and Biofilm-Eradicating Agents Accessed through a Modular Wohl-Aue Synthesis. Sci. Rep 2017, 7, 2003. [PubMed: 28515440]

(143). Garrison AT; Abouelhassan Y; Kallifidas D; Tan H; Kim YS; Jin S; Luesch H; Huigens RW III. An Efficient Buchwald-Hartwig/Reductive Cyclization for the Scaffold Diversification of Halogenated Phenazines: Potent Antibacterial Targeting, Biofilm Eradication and Prodrug Exploration. J. Med. Chem 2018, 61, 3962–3983. [PubMed: 29638121]

(144). Abouelhassan Y; Zhang Y; Jin S; Huigens RW III. Transcript Profiling of MRSA Biofilms Treated with a Halogenated Phenazine Eradicating Agent: A Platform for Defining Cellular Targets and Pathways Critical to Biofilm Survival. Angew. Chem., Int. Ed 2018, 57, 15523–15528.

(145). Smith PA; Koehler MFT; Girgis HS; Yan D; Chen Y; Chen Y; Crawford JJ; Durk MR; Higuchi RI; Kang J; Murray J; Paraselli P; Park S; Phung W; Quinn JG; Roberts TC; Rougé L; Schwarz JB; Skippington E; Wai J; Xu M; Yu Z; Zhang H; Tan MW; Heise CE Optimized Arylomycins are a New Class of Gram-Negative Antibiotics. Nature 2018, 561, 189–194. [PubMed: 30209367]

(146). Pinchman JR; Boger DL Probing the Role of the Vancomycin E-ring Aryl Chloride: Selective Divergent Synthesis and Evaluation of Alternatively Substituted E-ring Analogues. J. Med. Chem 2013, 56, 4116–4124. [PubMed: 23617725]

(147). Okano A; Nakayama A; Schammel AW; Boger DL Total Synthesis of [Ψ[C(═NH)NH]Tpg4]Vancomycin and its (4-Chlorobiphenyl)methyl Derivative: Impact of Peripheral Modifications on Vancomycin Analogues Redesigned for Dual D-Ala-D-Ala and D-Ala-D-Lac Binding. J. Am. Chem. Soc 2014, 136, 13522–13525. [PubMed: 25211770]

(148). Okano A; Nakayama A; Wu K; Lindsey EA; Schammel AW; Feng Y; Collins KC; Boger DL Total Synthesis and Initial Evaluation of [Ψ[C(═S)NH]Tpg^4]Vancomycin, [Ψ[C(═NH)NH]Tpg^4]Vancomycin, [Ψ[CH_2NH]Tpg^4]Vancomycin, and Their (4-Chlorobiphenyl)methyl Derivatives: Synergistic Binding Pocket and Peripheral Modifications for the Glycopeptide Antibiotics. J. Am. Chem. Soc 2015, 137, 3693–3704. [PubMed: 25750995]

(149). Okano A; Isley NA; Boger DL Peripheral Modifications of [Ψ[CH2NH]Tpg4]Vancomycin with Added Synergistic Mechanisms of Action Provide Durable and Potent Antibiotics. Proc. Natl. Acad. Sci. U. S. A 2017, 114, E5052–E5061. [PubMed: 28559345]

(150). Okano A; Isley NA; Boger DL Total Synthesis of Vancomycin-Related Glycopeptide Antibiotics and Key Analogues. Chem. Rev 2017, 117, 11952–11993. [PubMed: 28437097]

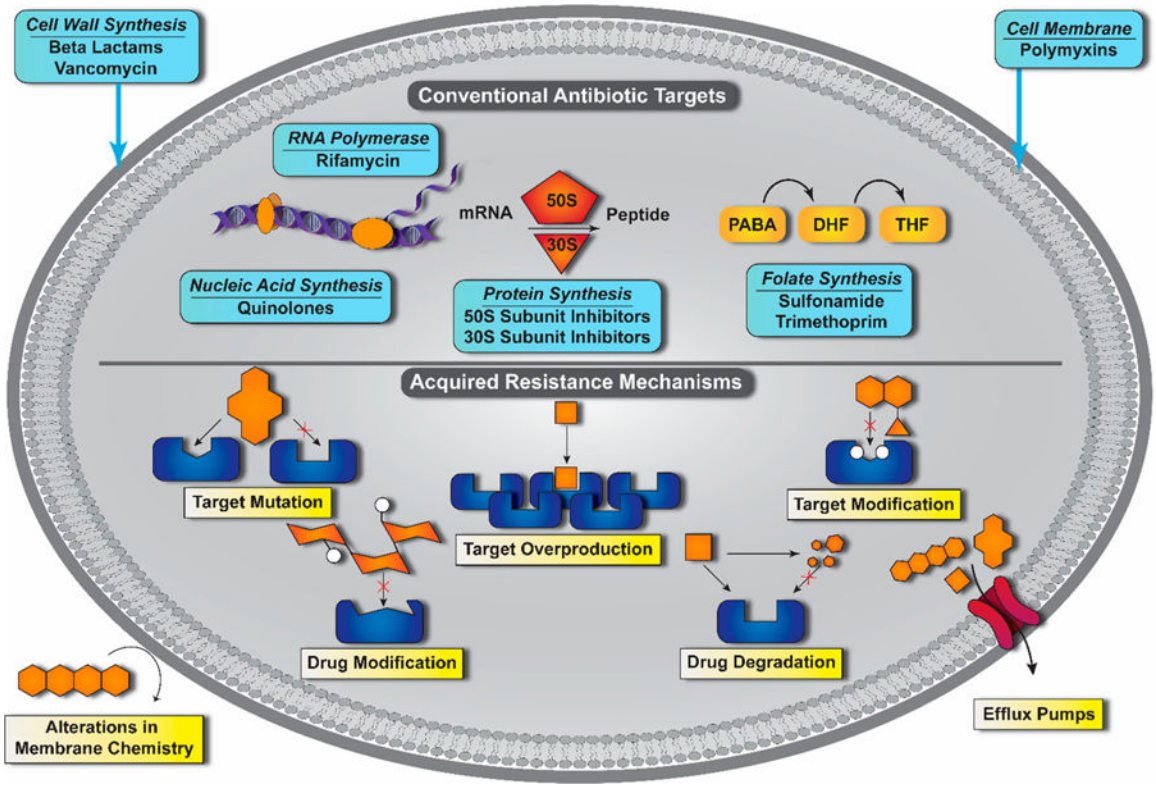

Figure 1.

Antibacterial targets of conventional antibiotics and mechanisms by which bacteria develop resistance to these therapeutic agents.

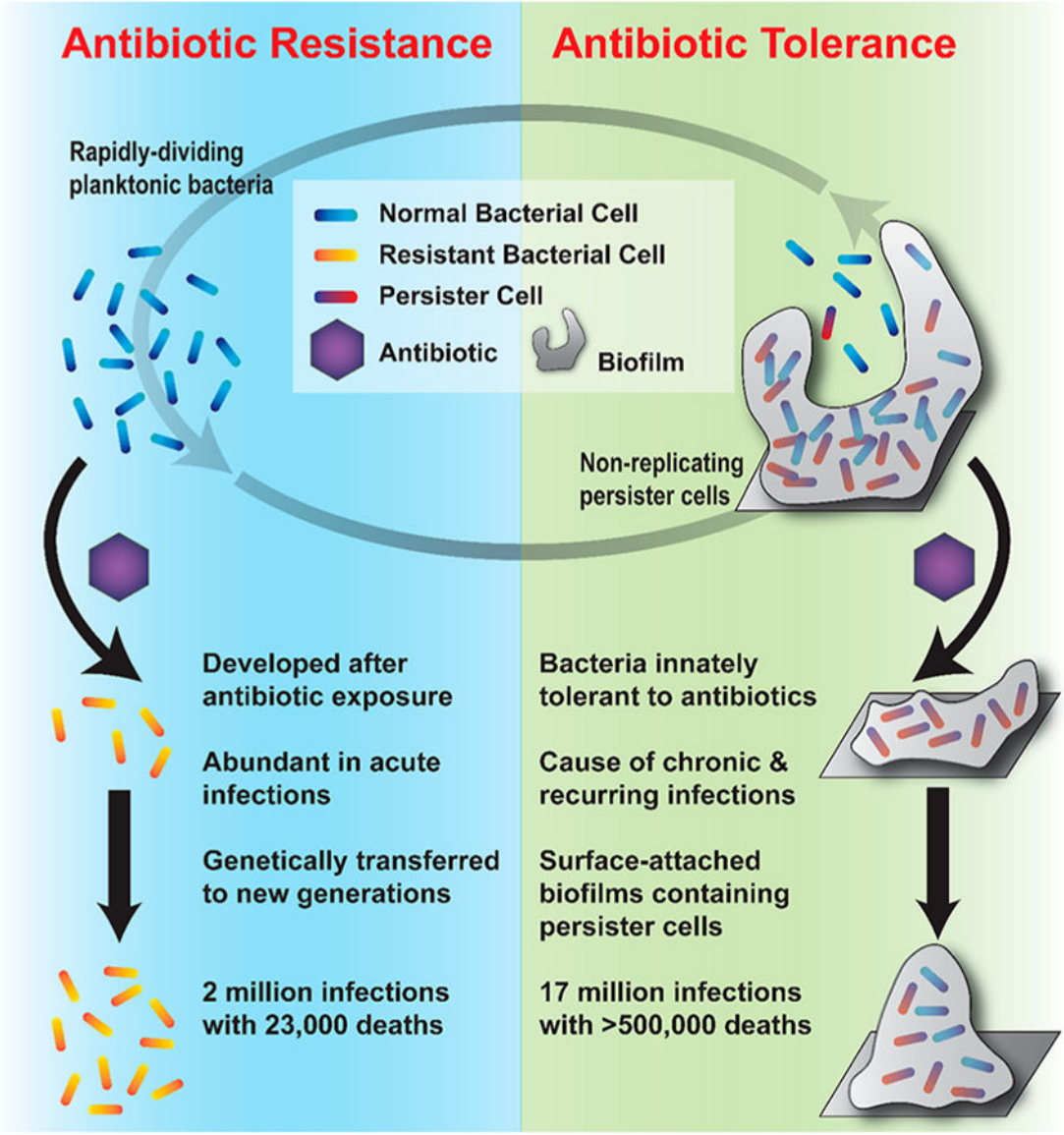

Figure 2.
Presentation of the distinctions between acquired antibiotic resistance and innate antibiotic tolerance.

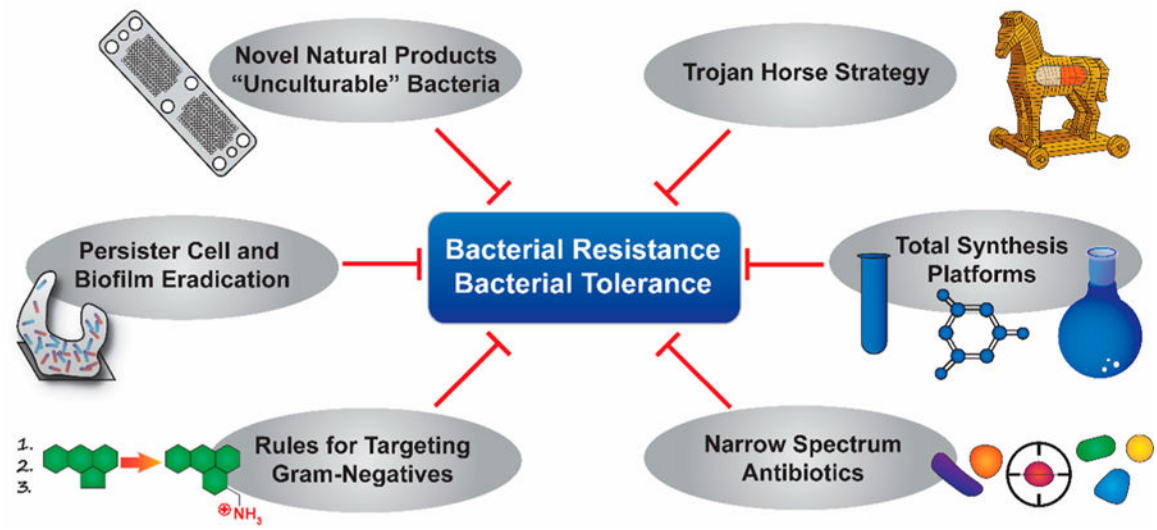

Figure 3.

Strategies to address the problems associated with antibiotic resistance and tolerance presented in this Perspective.

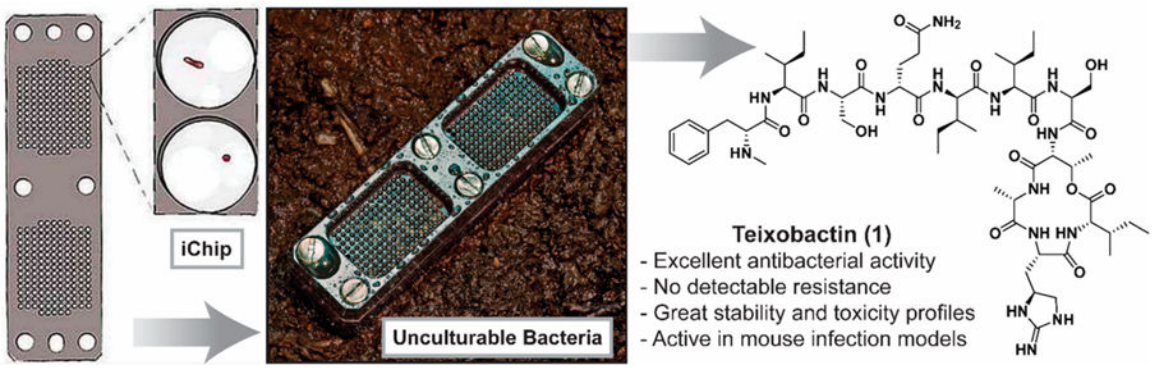

Figure 4.

iChip (multichannel device) technology developed by Lewis and co-workers to culture previously “unculturable” bacteria, which led to the discovery of the new antibiotic teixobactin **1**.

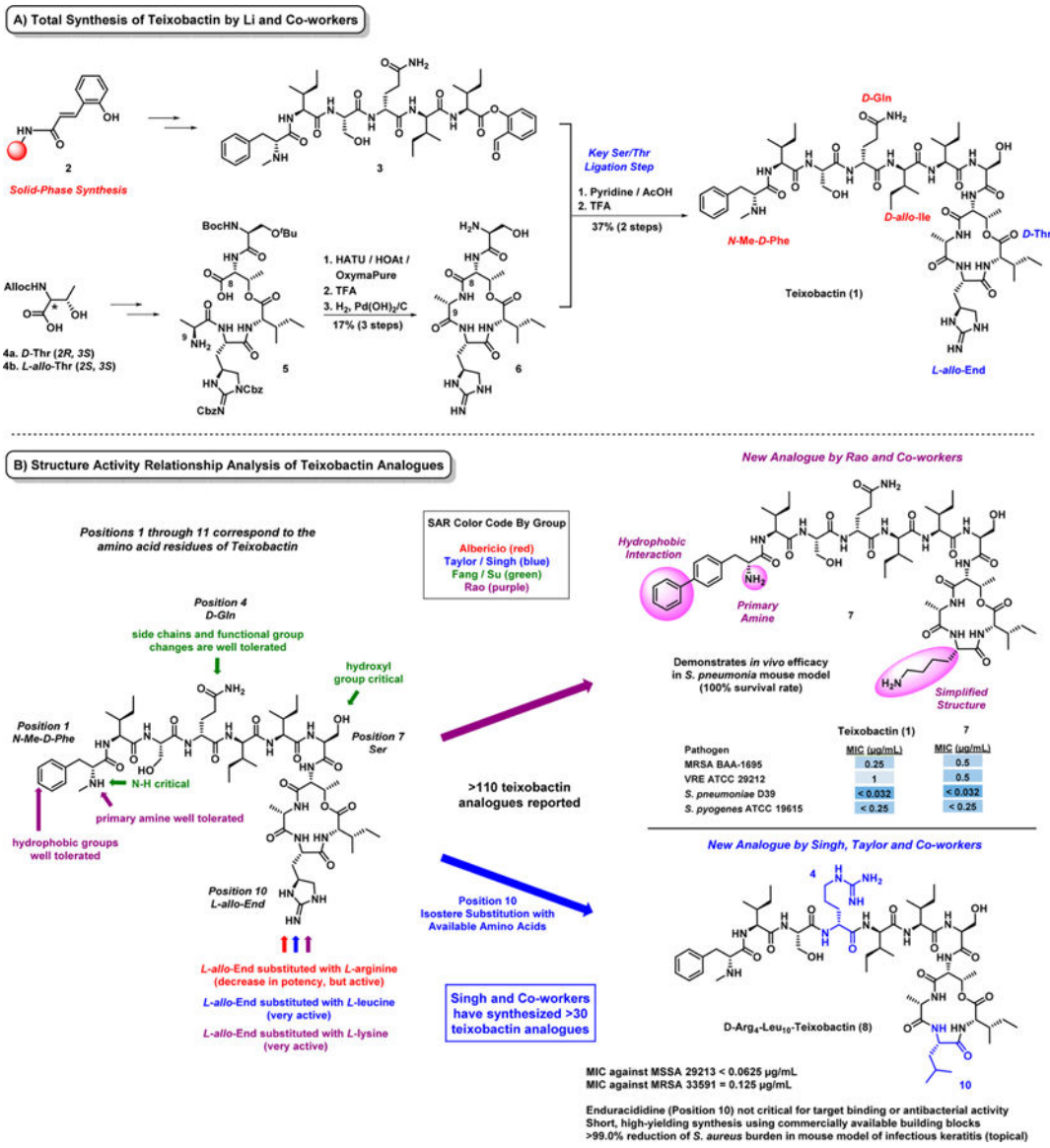

Figure 5.

(A) Total synthesis of the new antibiotic teixobactin **1** and (B) structure–activity relationship (SAR) insights.

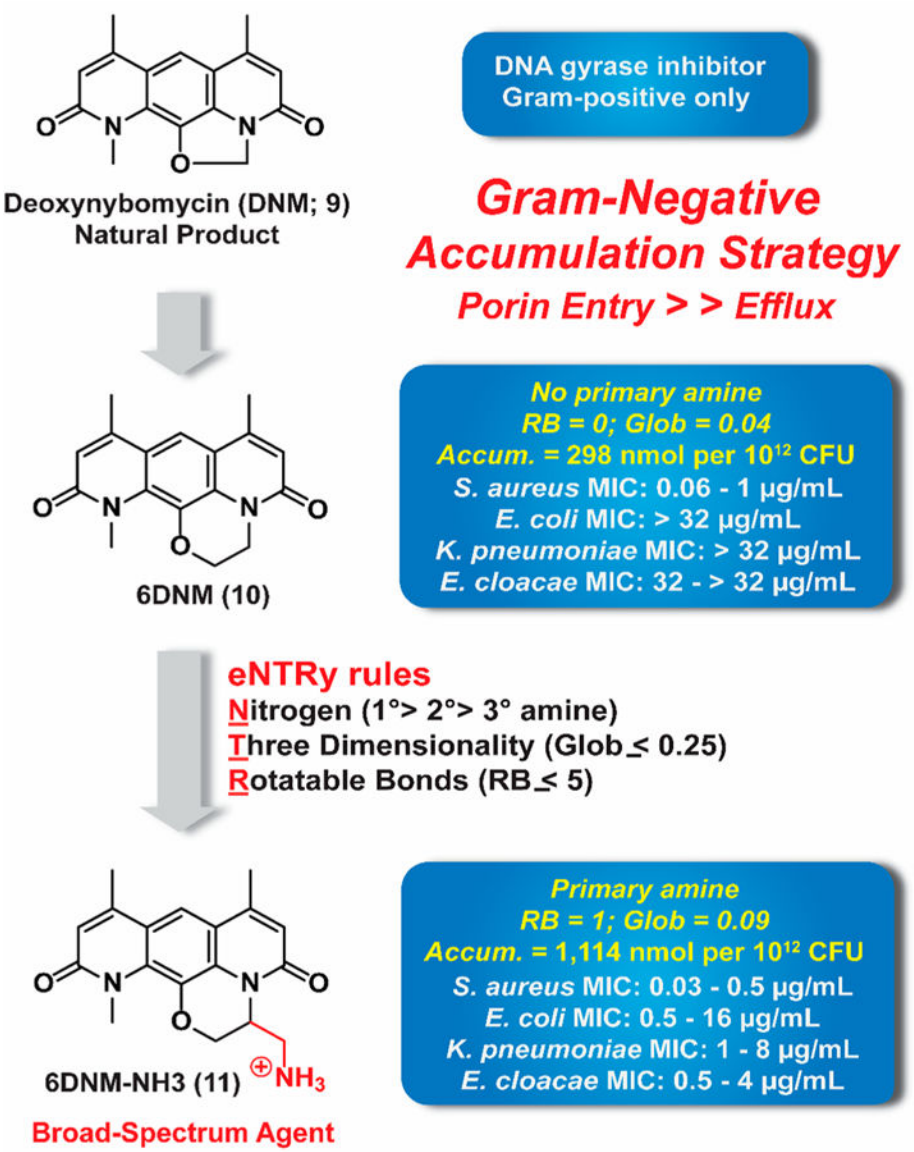

Figure 6.

eNTRy rules defined by Hergenrother and co-workers that enabled the successful conversion of the Gram-positive antibacterial agent 6DNM **10** into 6DNM-NH3 **11**, a new broad-spectrum antibacterial agent.

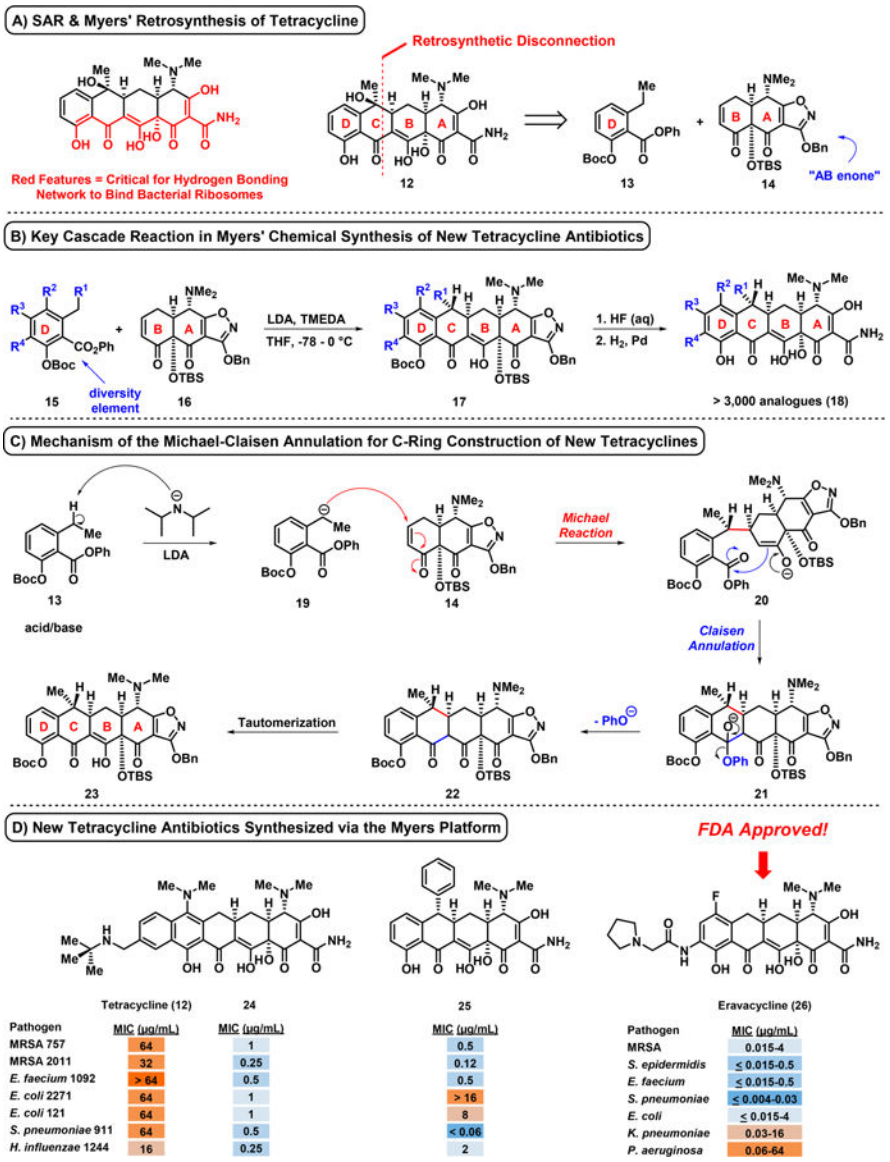

Figure 7.

(A) Myers' retrosynthetic analysis of tetracycline. (B) Key Michael–Claisen annulation step for fully synthetic tetracycline antibiotics. (C) Mechanism of Michael–Claisen annulation reaction. (D) Antibacterial profiles of fully synthetic tetracycline antibiotics, including FDA-approved eravacycline **26**.

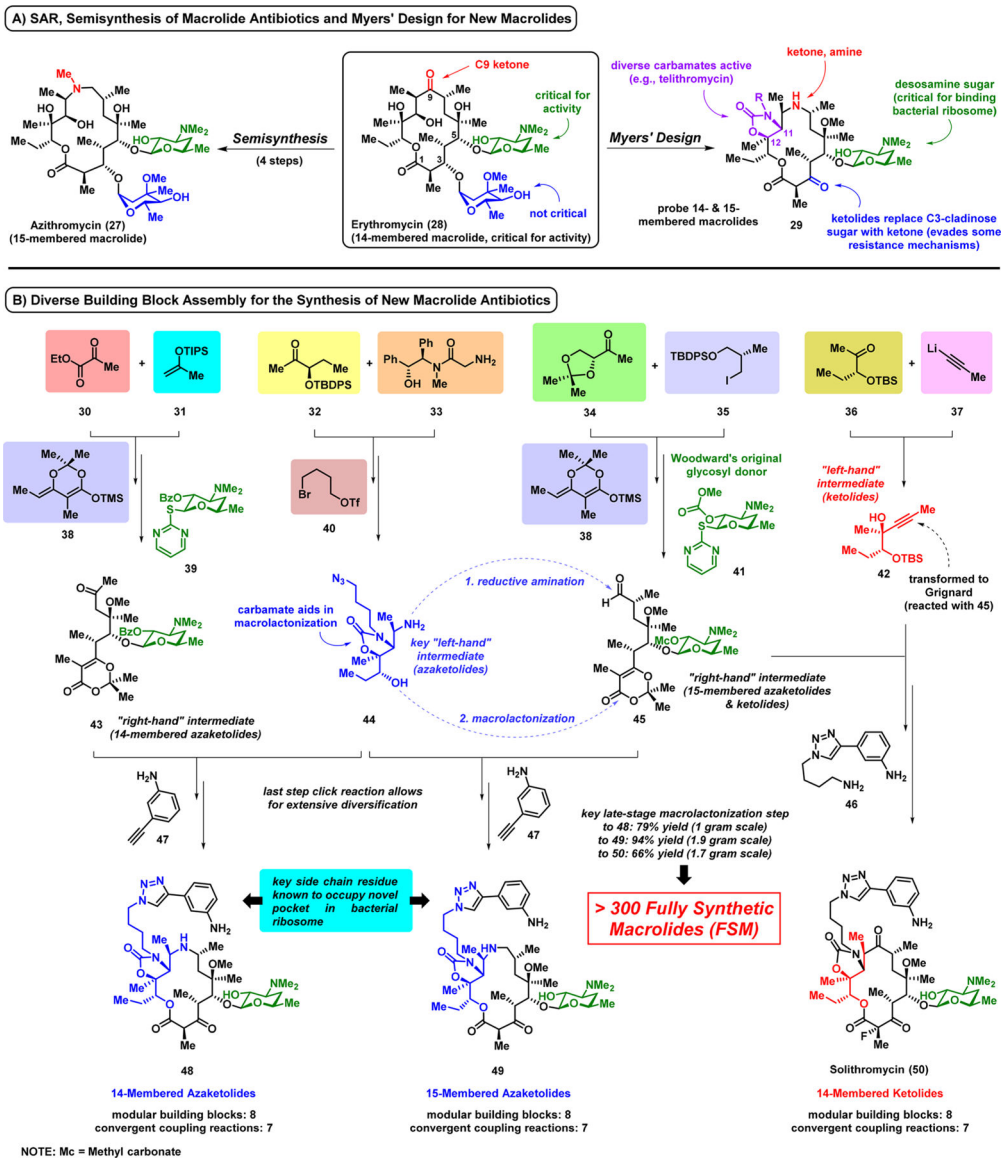

Figure 8.

(A) Overview of the structure–activity relationships related to macrolide antibiotics with Myers' design elements regarding new, fully synthetic macrolides. (B) Overview of the convergent chemical synthesis approach to access fully synthetic macrolide small molecules.

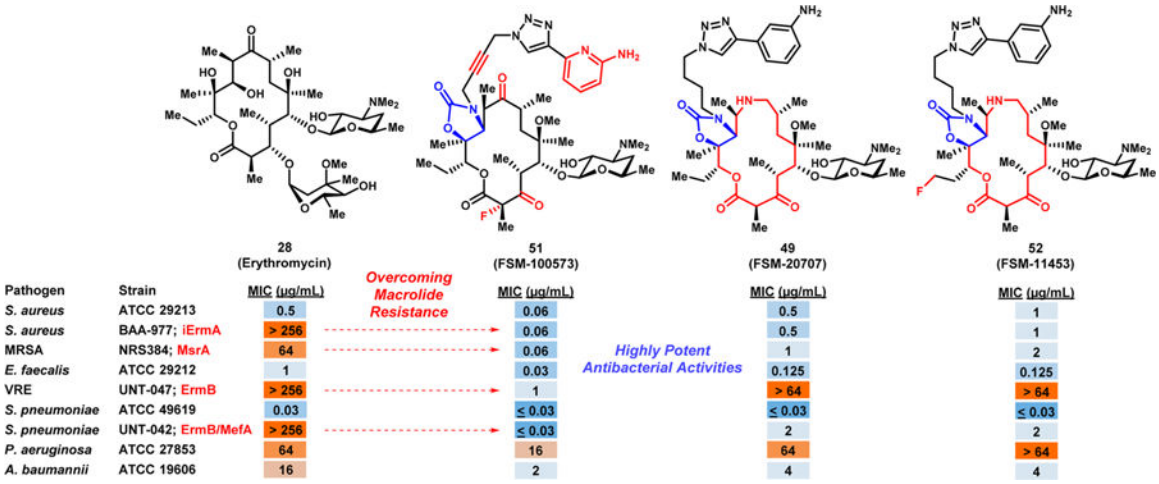

Figure 9.

Antibacterial profiles of select FSM analogues identified from microbiological studies. Several analogues demonstrate high antibacterial potencies and overcome specific macrolide resistance mechanisms. Resistant strain details are the following: iErmA, inducible erythromycin ribosome methyltransferase A; MsrA, macrolide streptogramin resistance efflux pump A; ErmB, erythromycin ribosome methyltransferase B; MefA, macrolide efflux protein A.

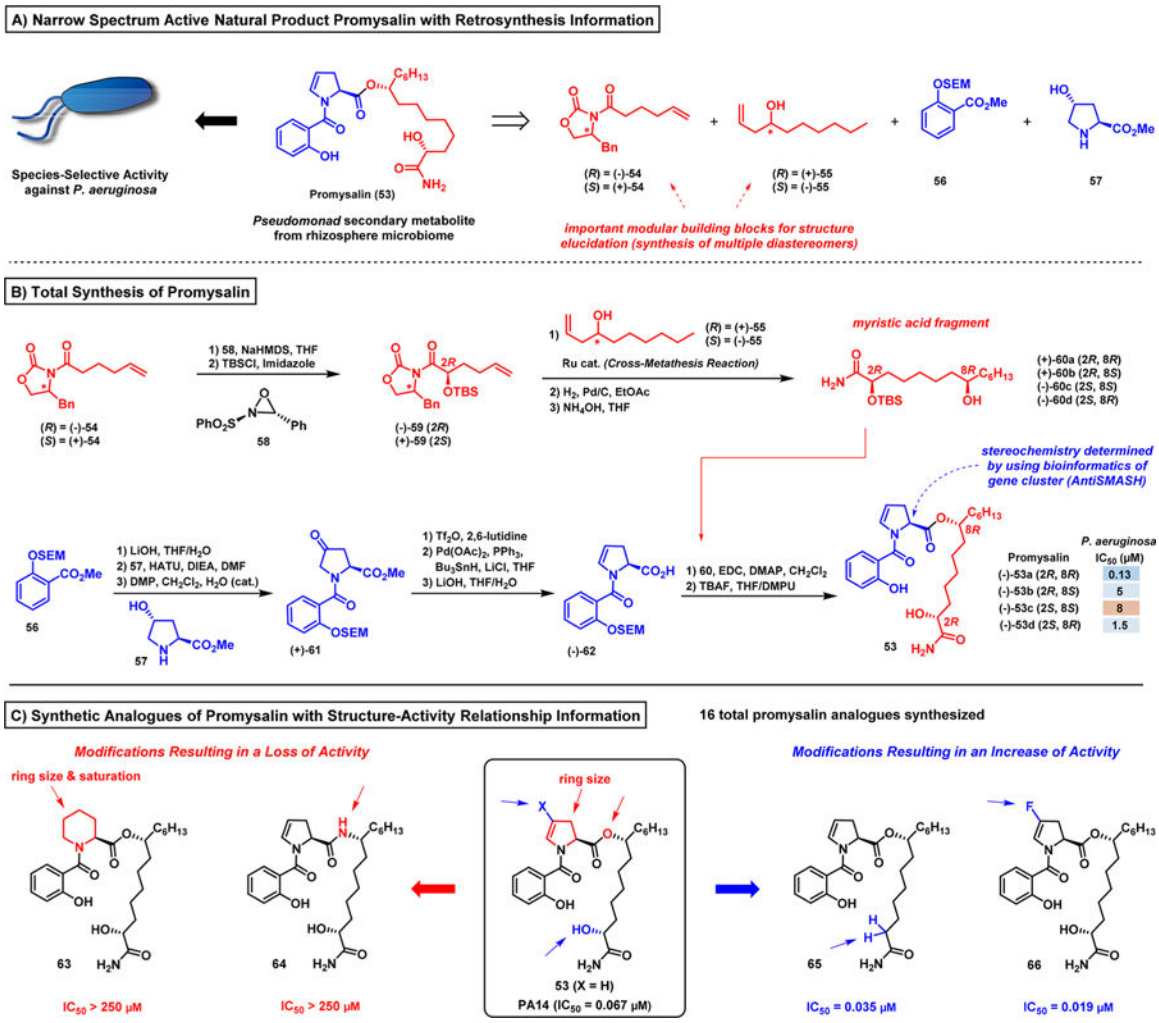

Figure 10.

(A) Retrosynthesis and (B) synthetic scheme to the *Pseudomonas aeruginosa* selective natural product promysalin by Wuest and co-workers. (C) Representative promysalin analogues synthesized using diverted total synthesis to probe structure–activity relationships against *P. aeruginosa* (strain *PA14*).

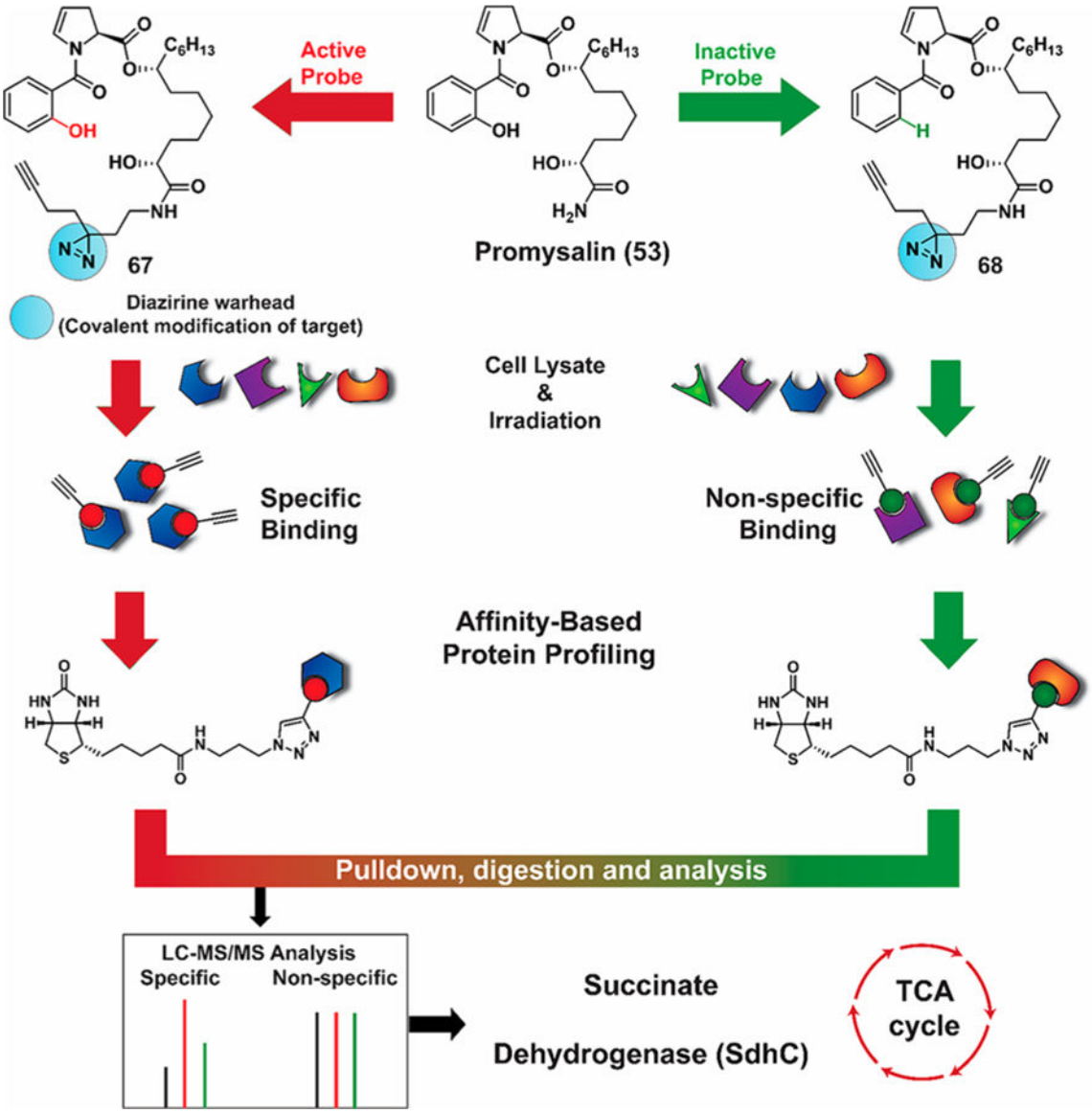

Figure 11.

Experimental workflow for pull-down experiments using photoactive diazirines **67** and **68** to identify succinate dehydrogenase (SdhC) as the biological target of species-specific antibiotic promysalin **53**.

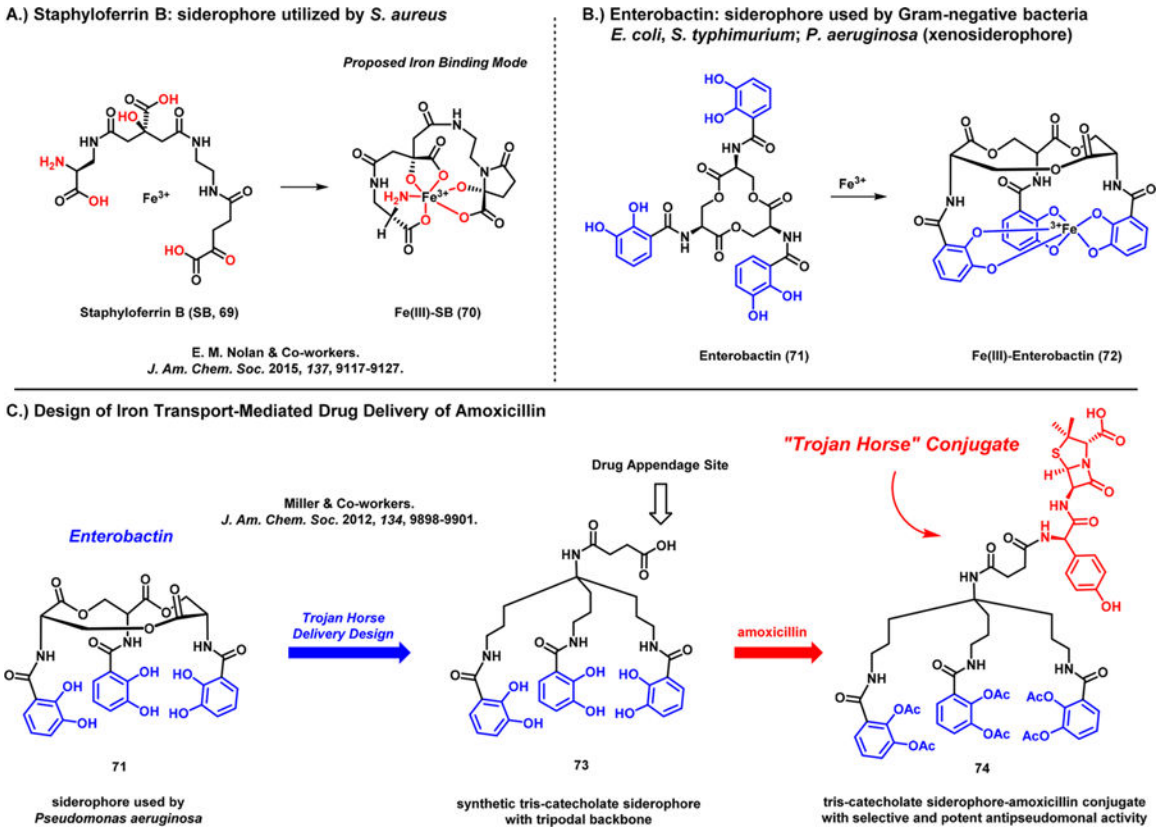

Figure 12.

(A) Structure and iron(III) complex with the *S. aureus* siderophore staphyloferrin B. (B) Enterobactin and iron(III) bound complex utilized by multiple Gram-negative pathogens for iron acquisition. (C) Utilization of iron uptake systems as a platform for antibiotic drug delivery by Miller and co-workers ("Trojan horse" conjugate **74** selectively and potently targets *P. aeruginosa* via iron uptake systems).

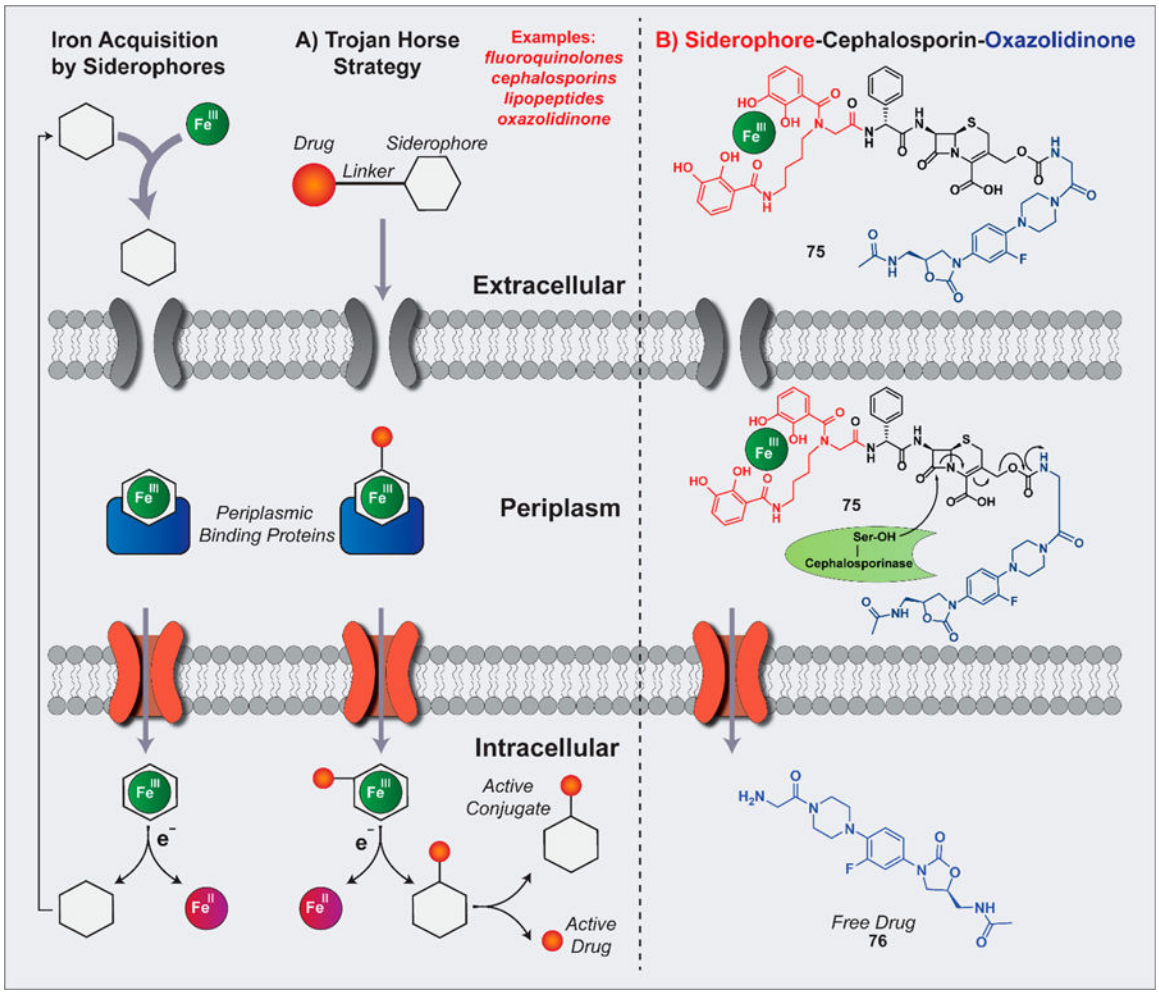

Figure 13.

(A) Illustration of the Trojan horse strategy for targeted antibiotic delivery. (B) Example of Trojan horse strategy with a suicide siderophore–cephalosporin–oxazolidinone **75** (via releasable linker) recently reported by Miller and co-workers.

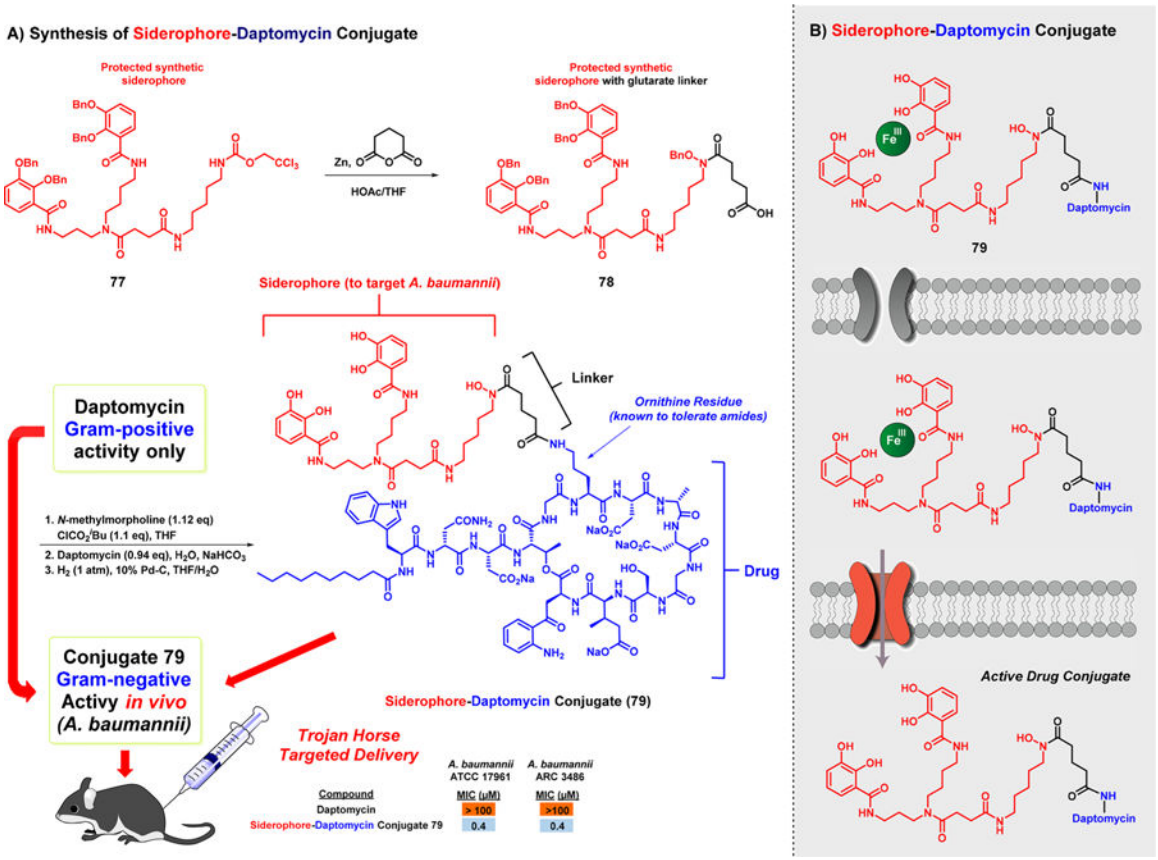

Figure 14.

Chemical synthesis and targeted *A. baumannii* activities of siderophore–daptomycin conjugate **79**.

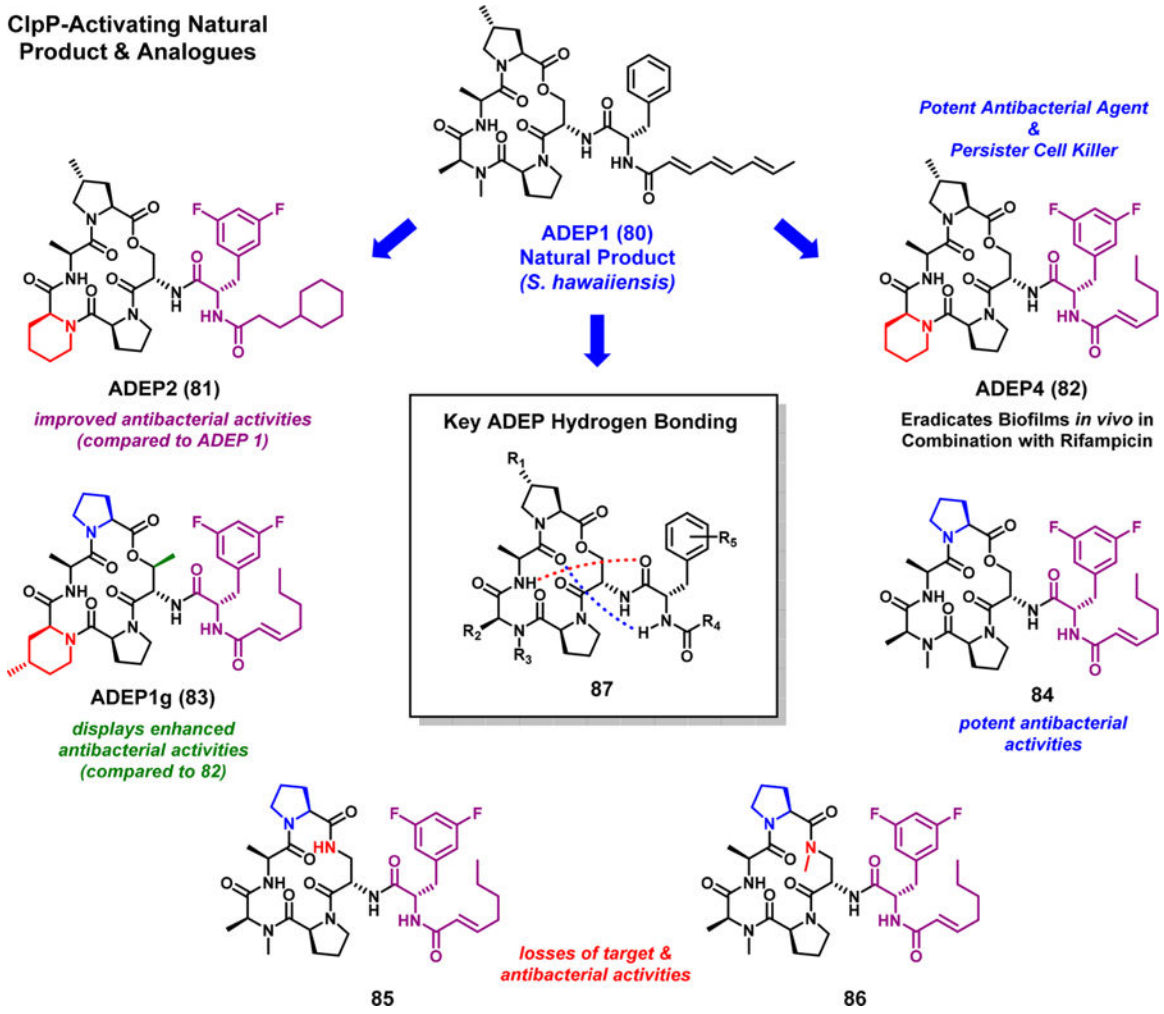

Figure 15.

Structures of the natural product, ADEP1 (**80**), its synthetic counterparts, and the key intramolecular hydrogen bonding required for activity. Structural modifications have been highlighted with different colors on each synthetic analogue.

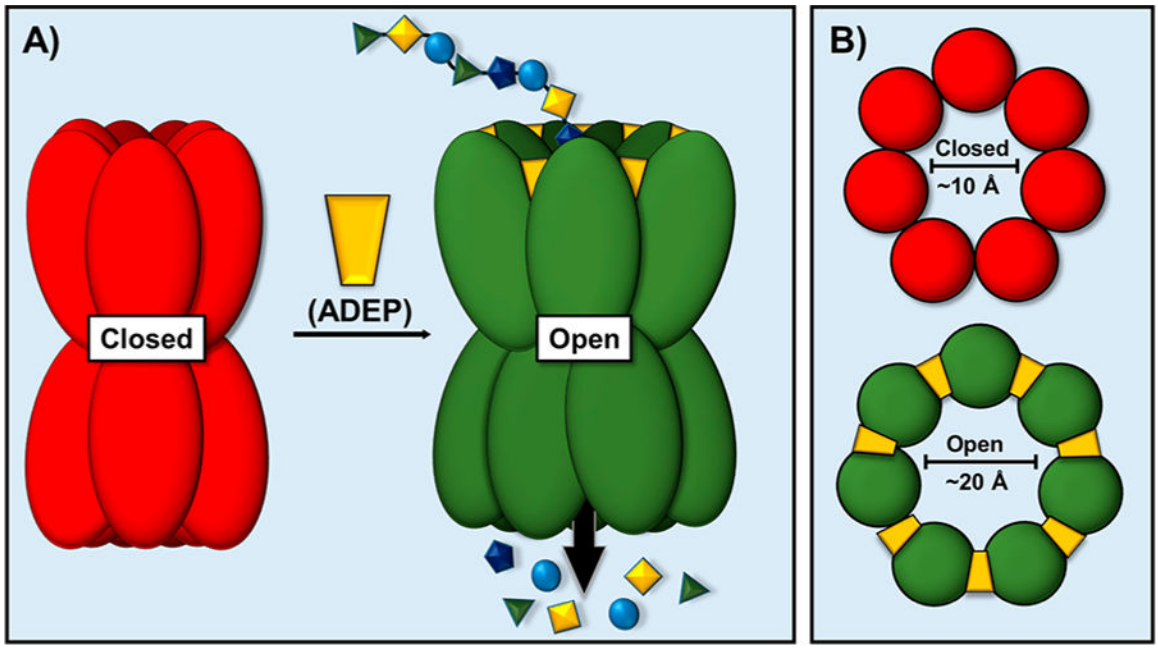

Figure 16.

(A) ADEPs bind to Clp-ATPase binding sites, promoting the entry of unfolded proteins into proteolytic sites, causing indiscriminate degradation of nascent polypeptides, ultimately leading to self-digestion and bacterial cell death. (B) The binding of ADEP analogues engenders the open conformation of the ClpP protease.

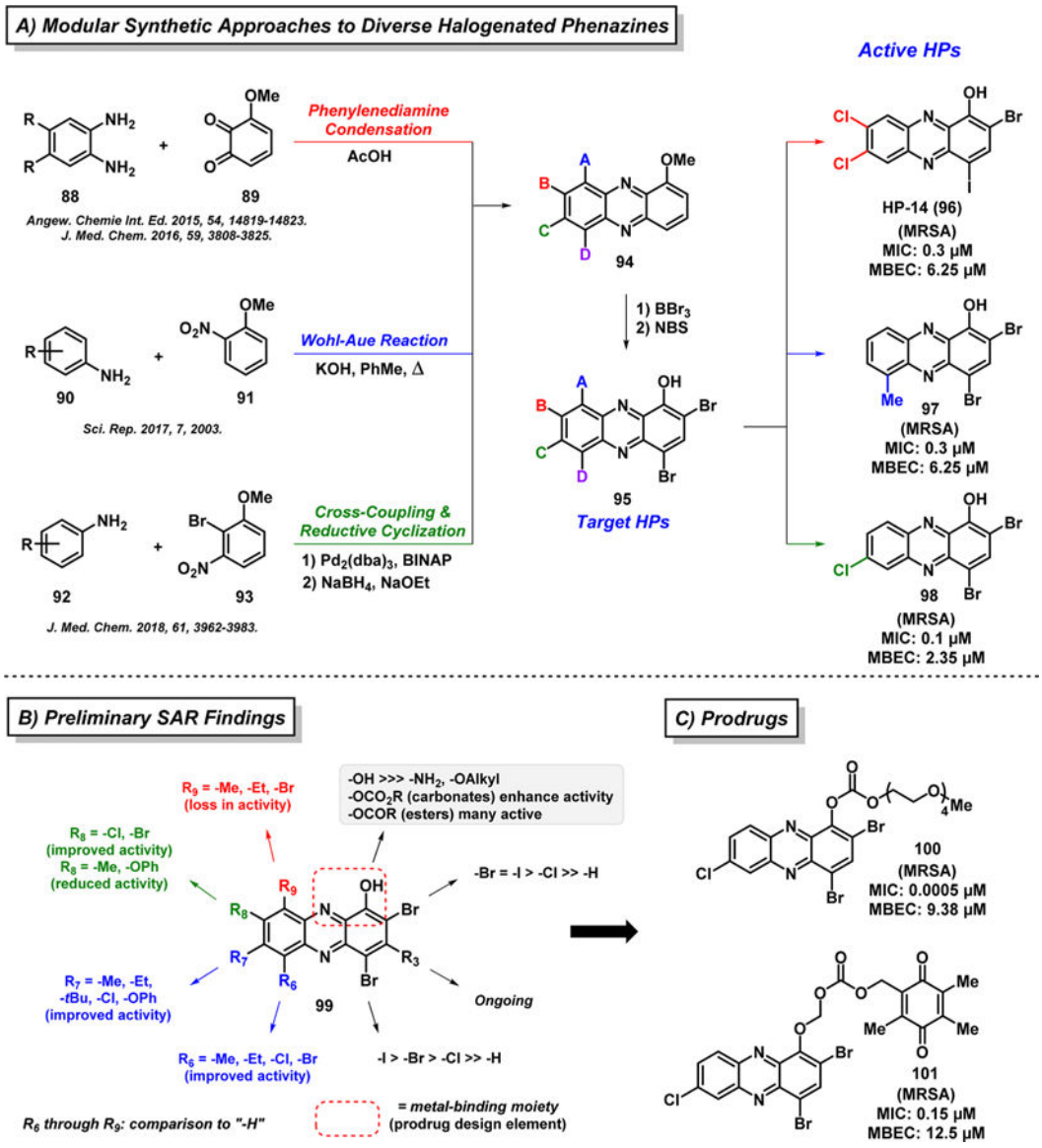

Figure 17.
Chemical synthesis of halogenated phenazines and preliminary SAR findings.

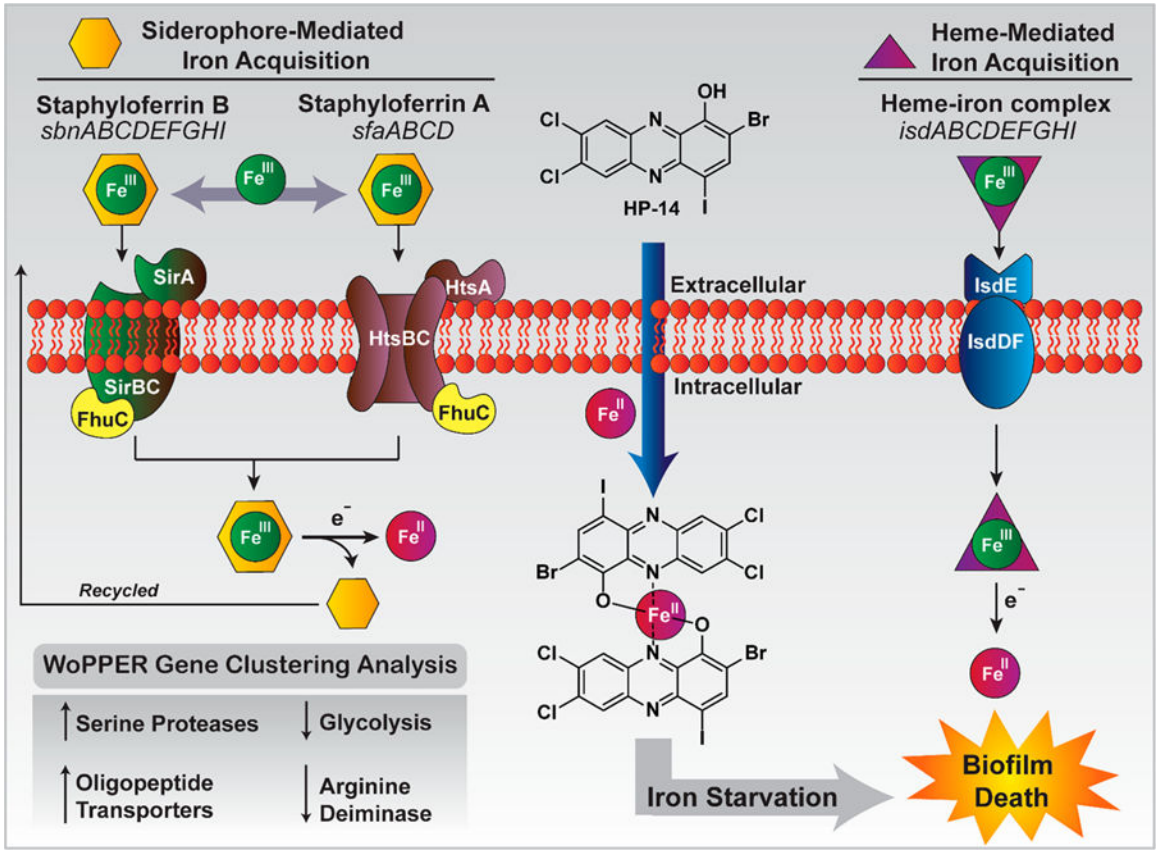

Figure 18.
Proposed mechanism of MRSA biofilm eradication by HP-14, based on RNA-seq findings.